# High-resolution Holocene record based on detailed tephrochronology from Torfdalsvatn, north Iceland, reveals natural and anthropogenic impacts on terrestrial and aquatic environments

David J. Harning[1,2], Christopher R. Florian[1,2,3], Áslaug Geirsdóttir[2], Thor Thordarson[2], Gifford H. Miller[1], Yarrow Axford[4], Sædís Ólafsdóttir[5]

[1]Institute of Arctic and Alpine Research, University of Colorado, Boulder, CO, USA
[2]Faculty of Earth Sciences, University of Iceland, Reykjavík, Iceland
[3]National Ecological Observatory Network, Battelle, Boulder, CO, USA
[4]Department of Earth and Planetary Sciences, Northwestern University, Evanston, IL, USA
[5]Reykjavík Energy, Reykjavík, Iceland

*Correspondence to*: David J. Harning (david.harning@colorado.edu)

**Abstract.** Open questions remain around the Holocene variability of climate in Iceland, including the relative impacts of natural and anthropogenic factors on Late Holocene vegetation change and soil erosion. The lacustrine sediment record from Torfdalsvatn, north Iceland, is the longest known in Iceland (~12000 cal a BP) and along with its high sedimentation rate, provides an opportunity to develop high-resolution quantitative records that address these challenges. In this study, we use two sediment cores from Torfdalsvatn to construct a detailed age model derived from marker tephra layers, paleomagnetic secular variation, and radiocarbon (20 age control points). We then apply this robust age constraint to support a complete tephrochronology (>2200 grains analyzed in 33 tephra horizons) and sub-centennial geochemical (MS, TOC, C/N, $\delta^{13}$C, and BSi) and algal pigment records (chlorins, lutein, diatoxanthin, and canthaxanthin). Along with previously published proxy records from the same lake, these records demonstrate generally stable terrestrial and aquatic conditions during the Early and Middle Holocene, except for punctuated disturbances linked to major tephra fall events. During the Late Holocene, there is strong evidence for naturally driven algal productivity decline beginning around 1800 cal a BP. These changes closely follow regional Late Holocene cooling driven by decreases in Northern Hemisphere summer insolation and the expansion of sea-ice laden Polar Water around Iceland. Then at 880 cal a BP, ~200 years after the presumed time of human settlement, a second shift in the record begins and is characterized by a strong uptick in landscape instability and possibly soil erosion. Collectively, the Torfdalsvatn record highlights the resilience of low-elevation, low-relief catchments to the pre-settlement soil erosion in Iceland, despite a steadily cooling background climate. The precisely dated, high-resolution tephra and paleoenvironmental record from this site can serve as a regional template for lowland regions of north Iceland.

**1 Introduction**

As the planet continues to warm, paleoclimate information is increasingly more important to constrain Earth system models (Tierney et al., 2020). Within the northern North Atlantic, Iceland serves as an ideal location for paleoclimate reconstructions as the island sits at the confluence of major atmospheric and oceanic circulation patterns integral to global heat distribution (Wunsch, 1980; Marshall et al., 2001). Continuous and high-resolution lake sediment records from Iceland form the backbone of its recent geologic climate history. These empirical records include physical properties for glacier history (Larsen et al. 2011; Striberger et al., 2012; Harning et al., 2016a, 2016b), pollen, macrofossils, and sedimentary ancient DNA (*sed*aDNA) for plant communities (Rundgren, 1995, 1998; Hallsdóttir and Caseldine, 2005; Gathorne-Hardy et al., 2009; Eddudóttir et al., 2015, 2016; Alsos et al., 2021; Geirsdóttir et al., 2022; Harning et al., 2023), bulk geochemistry for soil erosion and diatom productivity (Geirsdóttir et al., 2009, 2013, 2019, 2020, 2022; Larsen et al., 2012; Blair et al., 2015; Harning et al., 2018a; Tinganelli et al., 2018; Bates et al., 2021), lipid biomarkers for fire activity (Ardenghi et al., 2024), and chironomids and lipid biomarkers for quantitative temperature (Caseldine et al., 2003; Axford et al., 2007, 2009; Langdon et al., 2010; Holmes et al., 2013; Harning et al., 2020; Richter et al., 2020). The Holocene Thermal Maximum (7900 to 5500 cal a BP, Caseldine et al., 2006; Geirsdóttir et al., 2013) has been a particular focus as it provides a potential analogue for future environmental change – current estimates suggest that summer temperatures were ~3 ºC warmer than present (Flowers et al., 2008; Harning et al., 2020). As such, these proxy records have then been used to test and validate glacier models (Flowers et al., 2008; Anderson et al., 2018) and project future environmental scenarios (Anderson et al., 2019).

Research on Iceland's Holocene paleoclimate has also centered around the impact of human settlement during the last millennium. The classic paradigm is that following the settlement of Iceland (i.e., *Landnám,* ~870 CE, Vésteinsson and McGovern, 2012), soil erosion was intiated due to deforestation and overgrazing by newly introduced livestock (e.g., Thórarinsson, 1944, 1961; Dugmore and Buckland, 1991; Dugmore and Erskine, 1994; Hallsdóttir, 1995) with climate and volcanic forcings playing a secondary role (Thórarinsson, 1961; Gerrard, 1991). While human impact certainly affected the Icelandic landscape, empirical evidence demonstrates that the natural decline of woody vegetation (Streeter et al., 2015) and increased and sustained soil erosion began at least several centuries prior to known human presence (Geirsdóttir et al., 2009, 2020). These natural changes have been ascribed to Late Holocene cooling, due to diminishing Northern Hemisphere summer insolation and the southward migration of the Polar Front and sea ice towards Iceland (e.g., Axford et al., 2007; Geirsdóttir et al., 2013; Cabedo-Sanz et al., 2016; Harning et al., 2021), as well as volcanic eruptions whose tephra deposits initiate erosion through the abrasion and destruction of vegetation that stabilizes the underlying soil (Larsen et al., 2012; Geirsdóttir et al., 2013; Blair et al., 2015; Eddudóttir et al., 2017). Icelandic lake sediments provide optimal archives to explore the relationship and resilience of the landscape to climate and human impacts due to the lake's continuous sedimentation and high sedimentation rates. These conditions afford sub-centennial records of environment and climate variability and robust age control derived from geologically instantaneous tephra markers (e.g., Thórarinsson, 1944; Larsen and Eiríksson, 2008), among

other geochronological techniques (i.e., radioactive isotopes and paleomagnetic secular variations, PSV, Ólafsdóttir et al., 2013).

Icelandic volcanism has featured both effusive and explosive mafic eruptions during the Holocene, where the latter have often been influenced by frequent subglacial and subaqueous/submarine interactions resulting in considerable tephra production. Although less common, rhyolitic eruptions from central volcanoes are frequent in Iceland and typically more explosive than their mafic counterparts (e.g., Thordarson and Larsen, 2007; Thordarson and Höskuldsson, 2008; Larsen and Eiríksson, 2008). Due to their intensity, many of these rhyolitic eruptions have produced widespread, light-colored tephra layers that form the backbone of tephrochronological frameworks on both sides of the North Atlantic (e.g., Abbott and Davies, 2012; Lawson et al., 2012). Most Icelandic tephra layers have been dated in soil and sedimentary sections via radiocarbon ($^{14}$C) and soil/sediment accumulation rates (Mangerud et al., 1984, 1986; van den Bogaard et al., 1994, 2002; Dugmore et al., 1995; Pilcher et al., 1995, 1996; Birks et al., 1996; Wastegård et al., 2001; Langdon and Barber, 2001; Bergman et al., 2004; Óladóttir et al., 2005, 2007, 2011; Gudmundsdóttir et al., 2011, 2016, 2018; Timms et al., 2017, 2018; Harning et al., 2018b, 2019) in addition to annual layer counting in Greenland ice cores (Grönvold et al., 1995; Rasmussen et al., 2006; Davies et al., 2024). However, despite the vast existing literature and the high frequency of tephra-producing eruptions from Iceland during the Holocene (n ≈ 2400; Thordarson and Höskuldsson, 2008), the Icelandic record is incomplete due to a combination of preservation and the relatively few records with complete tephra layer inventories (e.g., Larsen et al., 2002; Thordarson and Larsen, 2007). Given Iceland's proximity to major regions of paleoenvironmental research, and the community's growing reliance on its tephra layers for age control and correlation between sites, continuing to work towards a well-dated and compositionally well-defined master tephra stratigraphy is paramount.

Here, we revisit the sediment of Torfdalsvatn, a lake in North Iceland (Fig. 1), to address several outstanding research gaps. Due to it being the only known non-marine sedimentary record in Iceland that extends to ~12000 cal a BP, Torfdalsvatn's lacustrine record has attracted considerable attention (e.g., Björck et al., 1992; Rundgren, 1995, 1998; Rundgren and Ingólfsson, 1999; Florian, 2016; Alsos et al., 2021; Harning et al., 2024). Important contributions include the major elemental composition of regional marker tephra layers (Björck et al., 1992; Alsos et al., 2021), which for the Early Holocene section have been recently revised (Harning et al., 2024). In addition, several paleoenvironmental records have been developed using pollen, macrofossils, chironomids, and plant *sed*aDNA to explore questions related to the postglacial colonization of plants and Holocene temperature variability (Björck et al., 1992; Rundgren, 1995, 1998; Axford et al., 2007; Alsos et al., 2021). However, currently, there has been no systematic study of all tephra layers preserved in Torfdalsvatn's sediment record and the response of the lake's aquatic environment to Holocene climate change has not been thoroughly explored. Therefore, in this study, we first use two lake sediment cores from Torfdalsvatn to construct a high-resolution age model derived from historical marker tephra layers, paleomagnetic secular variation, and radiocarbon. We then apply this robust age constraint to support a detailed tephrochronology (>2200 grains analyzed in 33 tephra horizons) and sub-centennial geochemical (MS, TOC, C/N, $\delta^{13}$C, and BSi) and algal pigment proxy records. Collectively, and along with previously published proxy records from

Torfdalsvatn, these new terrestrial and aquatic records provide key insight into the paleoenvironmental history of North Iceland during the Holocene and serve as a key tephrochronological and paleoenvironmental template for this region of Iceland.
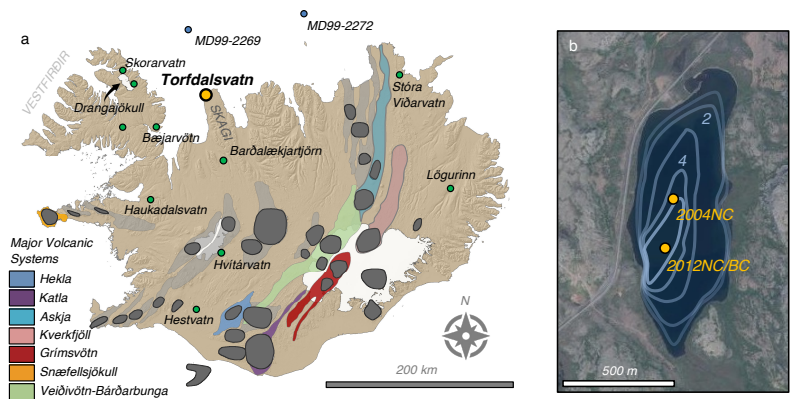
110 **Figure 1: Overview map of Iceland. a) Locations of major volcanic systems (dark gray denotes central volcano and color corresponds to volcanic system IDs in the legend), and terrestrial (green) and marine sites (blue) mentioned in the text, with Torfdalsvatn highlighted in yellow. b) Close-up of Torfdalsvatn, its bathymetry (1-m isolines), and location of lake sediment core sites for 2012NC (this study), 2012 BC (Harning et al., 2024), and 2004NC (Axford et al., 2007). Base aerial imagery courtesy of Loftmyndir ehf.**

115 ## 2 Methods

### 2.1 Study site and sediment core collection

Torfdalsvatn (66.06°N, 20.38°W) is a relatively small (0.4 km$^2$), shallow (5.8 m depth) lake located at 52 m asl on the northwest coast of the Skagi peninsula with a catchment area of 2.76 km$^2$ (Fig. 1). The surrounding bedrock is composed of Pliocene-Pleistocene age (3.3 to 0.8 Ma) basaltic lava successions separated by thin sedimentary units (Harðarson et al., 2008). Soils

120 within the low-relief lake catchment are thin and sparse, but where present, are composed of brown to histic andosols as well as some peat (Arnalds and Gretarsson, 2001). Our summer field visits indicate that the modern vegetation is broadly characterized as moss heathland.

In February 2012, we recovered lake sediment cores from the lake's depocenter using a Nesje piston coring system atop a lake-ice platform. We captured ~8.4 m of continuous sediment in two successive drives (TORF12-2A-1N and TORF12-

125 2A-2N; referred to as 2012NC) reaching dense, deglacial sediment at the base (Fig. 1b, note: another core 2012BC was taken from the same location, Harning et al., 2024). The cores were split and measured for density and magnetic susceptibility at 2-cm resolution on a GEOTEK (MSCL-S) core scanner at the University of Iceland. Here, we also present new tephra
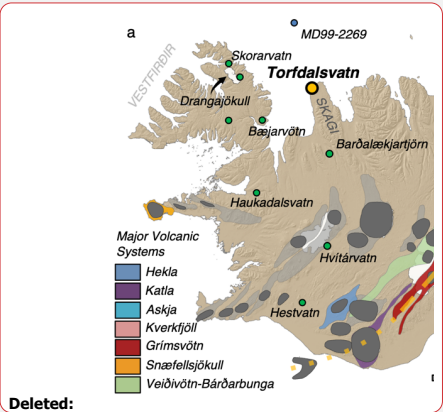
130  compositional data from a 5.4 m-long sediment record collected from a shallower water depth in February 2004 (04-TORF-01, i.e., 2004NC, Fig. 1b) previously studied for chironomid assemblages (Axford et al., 2007).

## 2.2 Tephra sampling and compositional analysis

Tephra layers from 2012NC and 2004NC were located by visual inspection (or high MS values for those that are not visible, i.e., cryptotephra) (Fig. 2) and sampled along the vertical axis. For the ~26 cm thick G10ka Series unit in 2012NC, samples

135  were taken every 1 cm. Each sample was sieved to isolate glass fragments between 125 and 500 μm and embedded in epoxy plugs. Tephra glass from 2012NC along with some layers from 2004NC were analyzed at the University of Iceland on a JEOL JXA-8230 electron microprobe using an acceleration voltage of 15 kV, beam current of 10 nA and beam diameter of 10 μm (see Supporting Data). The international A99 standard was used to monitor for instrumental drift and maintain consistency between measurements (see Supporting Data).

140      Using the compositional dataset, tephra layer origins were then assessed following the systematic procedures outlined in Jennings et al. (2014) and Harning et al. (2018b). Briefly, based on $SiO_2$ wt% vs total alkali ($Na_2O+K_2O$) wt%, we determine whether the tephra volcanic source is mafic (tholeiitic or alkalic), intermediate and/or rhyolitic. From here, we objectively discriminate the source volcanic system through a detailed series of bi-elemental plots produced from available compositional data on Icelandic tephra (see Supporting Data and Figs. S1-3). Merging the volcanic system source with relevant stratigraphic

145  and chronologic information permits the identification of the source eruption if the eruption is previously known. If a tephra horizon conforms to the composition of tephra of known age, then it forms a fixed point in the age model (i.e., marker tephra layer). If this is not possible, then an age is extracted from the age model (see Section 2.3.3) and named according to its volcanic source and modeled time of deposition. As an example, the Katla tephra layer identified at 142.5 cm depth (1270 cal a BP) is termed "Katla 1270" (Table 2). However, tephra layers from the historical period are classically labeled as age CE,

which          we          specify          where          needed.

155
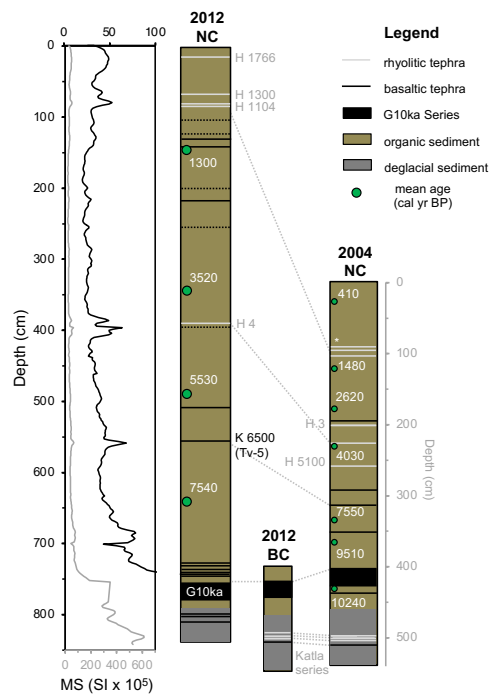
**Figure 2: Physical and lithological characteristics of Torfdalsvatn lake sediment. Magnetic susceptibility (MS, black and gray are two different scales) record and simplified lithostratigraphy shown for core 2012NC (this study), and lithostratigraphy for cores 2012BC (Harning et al., 2024) and 2004NC (Axford et al., 2007). Note that the 2004NC log is plotted on its own depth axis (gray). See Fig. 8 for stratigraphic detail of the Hekla 1104 CE tephra layers in core 2004NC. Key marker tephra** layers **are labeled in each core, and tephra layer correlations between records are highlighted with dashed gray lines. Depth and mean calibrated $^{14}$C ages of macrofossils samples shown for 2012NC and 2004NC with green circles. See Table 1 for complete radiocarbon information.**

160

**Table 1: Lake sediment radiocarbon information used in this study. All calibrated ages use the most recent radiocarbon calibration curve (IntCal20, Reimer et al., 2020).**

| Lab ID | Core name | Depth (cm) | Material | Conventional $^{14}$C age ± σ | Calibrated age BP ± σ | Reference |
|---|---|---|---|---|---|---|
| CURL-15806 | 2012NC | 148 | Aquatic macrofossil | 1390 ± 15 | 1300 ± 10 | This study |

| | | | | | | |
|---|---|---|---|---|---|---|
| CURL-15814 | 2012NC | 347 | Aquatic macrofossil | $3305 \pm 15$ | $3520 \pm 40$ | This study |
| CURL-15812 | 2012NC | 489.5 | Aquatic macrofossil | $4785 \pm 20$ | $5530 \pm 50$ | This study |
| CURL-15794 | 2012NC | 642 | Aquatic macrofossil | $6660 \pm 20$ | $7540 \pm 30$ | This study |
| AA60639 | 2004NC | 27.5 | Plant macrofossil | $370 \pm 40$ | $410 \pm 80$ | Axford et al. (2007) |
| NSRL-14520 | 2004NC | 120 | Plant macrofossil | $1635 \pm 20$ | $1480 \pm 60$ | Axford et al. (2007) |
| NSRL-14765 | 2004NC | 180 | Humic acid | $2515 \pm 20$ | $2620 \pm 100$ | Axford et al. (2007) |
| NSRL-14517 | 2004NC | 227.5 | Humic acid | $3685 \pm 15$ | $4030 \pm 50$ | Axford et al. (2007) |
| NSRL-14519 | 2004NC | 337.5 | *Betula* leaf | $6690 \pm 20$ | $7550 \pm 30$ | Axford et al. (2007) |
| NSRL-14766 | 2004NC | 369 | Humic acid | $8505 \pm 15$ | $9510 \pm 20$ | Axford et al. (2007) |
| NSRL-14518 | 2004NC | 432 | Humic acid | $9100 \pm 25$ | $10240 \pm 10$ | Axford et al. (2007) |

### 2.3 Chronology

### 2.3.1 Paleomagnetic secular variation

Continuous u-tube channels of sediment were taken from the center of core 2012NC and measured for paleomagnetic secular variation (PSV) following the methods of Ólafsdóttir et al. (2013). Torfdalsvatn's distinct characteristic remanent magnetization (ChRM) declination and inclination features were tuned to the master GREENICE PSV stack through 14 tie points (Fig. S4). The GREENICE chronology is based on 47 ^{14}C dates derived from two PSV-synchronized marine sediment cores (MD99-2269 and MD99-2322, Stoner et al., 2007, 2013), in addition to eight marker tephra layers of known age (Kristjánsdóttir et al., 2007).

### 2.3.2 Radiocarbon

2012NC was inspected for aquatic plant macrofossils to provide additional chronological control. Aquatic plants are generally favorable for ^{14}C dating in Iceland as there is no hardwater effect in lakes and terrestrial macrofossils have longer transport times that may result in ages that are stratigraphically too old. The four aquatic macrofossil fragments picked from 2012NC (Fig. 2) were gently rinsed with deionized water to remove sediment and freeze-dried. Samples were given an acid-base-acid pretreatment (Bradley and Stafford, 1994) and graphitized at the University of Colorado Boulder, then measured by AMS at

the University of California Irvine. Conventional $^{14}$C ages were calibrated using OxCal 6.0 (Bronk Ramsey, 2009) and the IntCal20 calibration curve (Reimer et al., 2020), and are reported in cal a BP, where BP is years before present (1950 CE, Table 1).

190 **2.3.3 Age model**

The 2012NC age model relies on a combination of key marker tephra layers whose ages are known from the historical period (*n*=2, Hekla 1766 and Hekla 1300, e.g., Thórarinsson, 1967), PSV tiepoints (*n*=14), and $^{14}$C-dated macrofossils (*n*=4). An age model was generated using the open-source R package rbacon (Blaauw and Christen, 2011; R Core Team, 2021), the IntCal20 calibration curve for the $^{14}$C samples (Reimer et al., 2020), and an uncertainty of ± 50 cal a BP for each PSV tie point (e.g.,

195 Ólafsdóttir et al., 2013) (Fig. 3a). Given the thin nature of tephra layers typically less than 1 cm, we did not remove tephra layer thicknesses from the model. Non-marker tephra layer ages are derived from basal depth of the layer, the median value of model iterations (red line), and the 95% uncertainty envelope (grey lines) (Fig. 3a).
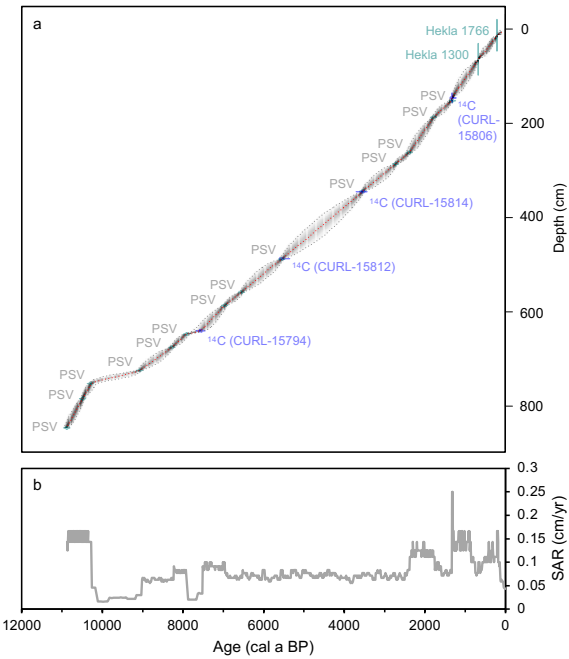
205

**Figure 3: Age model results. a)** rbacon age model constructed from the PSV tie points (gray, *n* = 14), historical marker tephra layers (green, *n* = 2), and radiocarbon ages of plant macrofossils (blue, *n* = 4) (Blaauw and Christen, 2011; R Core Team, 2021), where solid red line reflects the median of model iterations, and the outer gray lines reflect the 95% confidence envelope. See Fig S4 for PSV results. b) Sedimentation accumulation rates (SAR, cm/yr) derived from the rbacon age model.

## 2.4 Bulk geochemistry

210

Samples were taken for bulk geochemistry at 2-cm resolution (1-cm thick), avoiding tephra layers, then ground and homogenized with an agate mortar and pestle. Total carbon (TC), total nitrogen (TN), and δ¹³C (relative to VPDB) were measured using a CE NC 2500 elemental analyzer interfaced to a Finnigan Delta V isotope ratio mass spectrometer at the Carnegie Geophysical Laboratory. Isotopic ratios were corrected for drift using an acetanilide standard, and duplicate analyses

215 show a precision of less than 0.2 ‰ for each isotope ratio. For a subset of these samples (*n*=281), we also measured biogenic silica (BSi) by Diffuse Reflectance Fourier Transform Infrared Spectrometry (FTIRS) on a Bruker Vertex 70 with a Praying Mantis diffuse reflectivity accessory (Harrick) at the University of Colorado Boulder, integrating between 1000 and 1250 cm⁻¹. Since published calibrations to wt% biogenic silica are linear and do not influence the nature of the proxy curve (e.g., Vogel et al., 2008), we report values in FTIRS absorbance units. Previous studies in Iceland report low instrumental uncertainty for

220 this method (0.087 to 4.334 absorbance units, Harning et al., 2018a).

## 2.5 Algal pigments

Samples for algal pigments were taken at 2-cm resolution above 226 cm depth (~2000 cal a BP) and at 4-cm resolution below, where each corresponds to an interval previously sampled for bulk geochemistry as described above. Algal pigments were measured at the University of Colorado Boulder following the methodology described in Leavitt and Hodgson (2001) to

225 minimize pigment degradation. The archive half of sediment core was used for pigment analysis because it was sealed, stored cold, and not visibly oxidized at the time of sampling and all subsamples were kept frozen under nitrogen until the time of measurement. Briefly, following core splitting, algal pigments were immediately solvent extracted from 246 freeze dried sediment samples using 6 mL of acetone:methanol (80:20, v/v) overnight in amber vials under N₂ at -10 °C. Samples were touch mixed and sonicated to disperse sediment and increase extraction efficiency, then filtered through a 0.2 μm PTFE syringe

230 filter which was then rinsed with 2 ml of acetone to recover sample residue from the filter. The extract was dried down and rehydrated with a known volume of acetone containing a known concentration of α-tocopherol standard. Samples were placed in the refrigerated autosampler of an Agilent 1200 series HPLC and derivatized to improve chromatographic behavior immediately prior to injection with an equal volume of 28 mM tetrabutyl ammonium acetate in water. A binary mobile phase system was used with solvent A composed of methanol:28 mM tetrabutyl ammonium acetate (70:30, v/v) in water and solvent

235 B composed of pure methanol at a flow rate of 1 mL min⁻¹. An Agilent Eclipse XDB-C18 4.6 x 150 mm column was used to separate pigments whose absorbance of visible light was detected by an Agilent Diode Array Detector (DAD) scanning between 400 and 750 nm. Pigments were identified by comparing characteristic absorbance spectra with that stored in a library
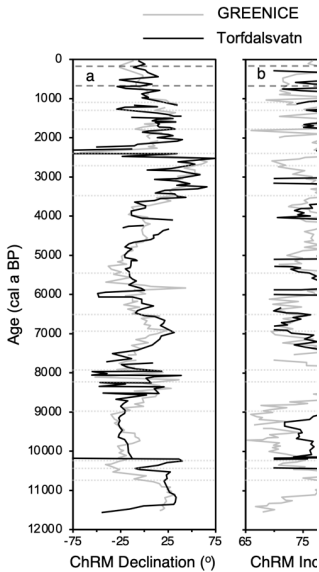
created from a suite of standards obtained from DHI Denmark and reported as concentration normalized to organic carbon (µg pigment/mg OC).

## 2.6 Statistics

To compare the (dis)similarity of different proxy records and reduce their overall dimensionality, we performed Principal Coordinate Analysis (PCoA) using a Bray-Curtis dissimilarity matrix on both the bulk geochemistry and algal pigment proxy datasets. Bulk geochemistry datasets include SAR, %TOC, C/N, $\delta^{13}$C, and BSi, but not MS due to the interference of tephra layers. Algal pigment datasets include total pigments, total chlorins, diatom pigments, lutein/diatoxanthin, and canthaxanthin. For each analysis, sample sets were reduced to the lowest common resolution. All analyses were performed in the open-source platform R (R Core Team, 2021) using the phyloseq package (McMurdie and Holmes, 2013).

## 3 Results

### 3.1 Tephra stratigraphy and age model

Torfdalsvatn's tephra stratigraphy is shown in Figure 2 and Table 2, where age and origin are indicated along with correlations between the 2012NC/BC and 2004NC cores. Detailed tephra layer descriptions ($n$ = 33), compositional datasets (>2200 grains analyzed), and elemental plots used to identify the tephra layers are provided in the Supporting Data and Information. We stress, unless otherwise noted, that our chemical data is obtained from pristine basaltic to silicic tephra grains that feature delicate protrusions (e.g., Harning et al., 2024). In samples regarded as representing pristine tephra fall, the grains in the mafic realm (basalt to andesite) range from (i) non- to poorly (<20 %) vesicular, black blocky glass grains defined by brittle fracture surfaces to (ii) poorly- to highly-vesicular (20 to 60 %) black to brown glass grains with vesicle-pitted surfaces to (iii) highly vesicular (>60 %) translucent (sideromelane), brown to pale brown glass grains with very convolute outlines to (iv) achneliths defined by coherent shiny black glazed/fused outer surfaces (e.g., Walker and Croasdale, 1972; Thordarson et al., 1996). The felsic (high-silica andesite, dacite to rhyolite) realm are highly vesicular (>60 %) grains and are either pumice fragments with irregular outlines or fragments dominated by tube-vesicles or vesicle-wall/bubble-junction glass shards (e.g., Fisher and Schmincke, 1984).

We identified 28 visible tephra and 5 cryptotephra horizons in the lake sediment of Torfdalsvatn. In total, these tephra horizons represent at least 78 separate fall events (Table 2) as the majority ($n$=24; 73%) feature tephra fall from more than one volcanic system. On 9 occasions (27%), the horizons contain tephra with composition indicating a single system as the source. Most common are tephra horizons with 2 source systems ($n$=13; 39%), then those with 3 source systems ($n$=8; 24%), followed by 4 ($n$=2; 6%) and then 7 ($n$=1; 3%). In 19 out of 24 (79%) tephra horizons, the tephra populations indicate additional source systems present as minor components, and in some instances only by a single grain. In 6 instances (18%), the different source system populations are present in more equal proportions and 4 of those cases (12%) are represented by the cryptotephra horizons. The source systems indicated are Grímsvötn ($n$=31; 40%), Hekla ($n$=17; 22%), Katla ($n$=14; 19%), Veiðivötn-

Bárðarbunga (*n*=7; 9%), Askja (*n*=3; 4%), Kverkfjöll (*n*=3; 4%), and unknown (*n*=2; 3%) (SDT2). All these systems are distal to Torfdalsvatn, where Katla is farthest away (~270 km) and Askja is closest (~200 km). Consequently, only the more powerful explosive eruptions at these systems had the potential to produce tephra fall at Torfdalsvatn. Please see Supporting Information for more details on the implications of Torfdalsvatn's tephra stratigraphy.

The age model for core 2012NC uses 2 historic marker tephra layers of well-established age (Hekla 1766 and Hekla 1300, Thórarinsson, 1967), 14 PSV tiepoints, and 4 $^{14}$C-dated macrofossils (Fig. 3a). With the lowest PSV tie point assigned to an age of 10868 cal a BP, the high density of chronological control points (*n* = 20) results in an average of about 1 every 500 years. The fact that $^{14}$C-dated macrofossils CURL-15814 (3520 ± 40 cal a BP, 347 cm depth) and CURL-15812 (5530 ± 50 cal a BP, 489.5 cm depth) are statistically identical to neighboring PSV tie points at 346 (3523 cal a BP) and 490 cm depth (5531 cm depth) highlights the strong compatibility of these independent dating techniques for the Torfdalsvatn sediment record (Fig. 3). Combined with the Bayesian modeling approach, the age model therefore provides relatively precise estimates on the ages of new tephra layers as well as the timing of past paleoenvironmental change derived from proxy records (e.g., Blaauw et al., 2018). Based on this age model, sedimentation accumulation rates (SAR) have minimal variation throughout the entirety of the Holocene record (Fig. 3b), particularly compared to SARs of other non-glacial lakes in Iceland (e.g., Geirsdóttir et al., 2013). Due to the near linear sedimentation rate, we do not present the following proxy data as fluxes as this results in negligible changes to the structure of proxy records.

**Table 2: Summary of Torfdalsvatn tephra stratigraphy and chronology. See Supporting Data for major element compositions and chemical identification of the tephra layers.**

| Tephra ID | Dominant composition | Cumulative depth (cm)[1] | Thickness (cm) | Age (cal a BP) | Number of events[3] |
|---|---|---|---|---|---|
| Hekla 1766* | Rhyolite to icelandite | 15 | 0.1 | 184 | 3 |
| Hekla 1300* | Rhyolite to icelandite | 66 | 0.1 | 650 | 3 |
| **Hekla 1104*** | Rhyolite | 84 | 0.7 | 846 | 3 |
| Cryptotephra 990 | Mix | 104 | - | 990 ± 80 | 4 |
| Cryptotephra 1180 | Mix | 125 | - | 1180 ± 70 | 2 |
| Katla 1220 | Alkali basalt | 131 | 1 | 1220 ± 50 | 3 |
| Katla 1270 | Alkali basalt | 142.5 | 2 | 1270 ± 40 | 2 |
| Cryptotephra 1850 | Mix | 202 | - | 1850 ± 50 | 3 |
| Katla/Grímsvötn 1990 | Mix | 219 | 0.4 | 1990 ± 140 | 3 |
| Cryptotephra 2320 | Mix | 257 | - | 2320 ± 70 | 4 |
| Hekla C* | Icelandite | ~340 | 0.5 | 2800 ± 80 | 2 |
| **Hekla 3*** | Icelandite, rhyolite | ~349 | 2 | 3060 ± 30 | 2 |
| Hekla 4* | Rhyolite | 391 | 1.3 | 4260 ± 10 | 2 |
| Hekla 4270 | Alkali basalt | 397 | - | 4270 ± 180 | 2 |
| **Hekla 5100** | Rhyolite and alkali basalt | ~450 | 0.8 | ~5100 | 1 |
| **Askja 5700** | Primitive basalt | ~505 | 0.1 | ~5700 | 1 |
| Kverkfjöll/Katla 5850 | Tholeiite basalt | 512 | 0.1 | 5850 ± 200 | 2 |
| **Katla 6500 (Tv-5)** | Alkali basalt | 557 | 1.1 | 6490 ± 130 | 1 |
| **Grímsvötn/Katla 8500** | Tholeiite/alkali basalt | 675 | 0.1-0.2 | ~8500 | 2 |
| Grímsvötn? 9260 | Tholeiite basalt | 730 | 0.3 | 9260 ± 300 | 1 |
| **Grímsvötn 9410 (G10ka Series #13)*** | Tholeiite basalt | 734 | 0.6 | 9410 ± 340 | 2 |

| | | | | | |
|---|---|---|---|---|---|
| **Grímsvötn 9630 (G10ka Series #12)*** | Tholeiite basalt | 739.5 | 1.1 | 9630 ± 350 | 1 |
| **Grímsvötn 9740 (G10ka Series #11)*** | Tholeiite basalt | 742.5 | 0.5 | 9740 ± 320 | 2 |
| **Grímsvötn 9850 (G10ka Series #10)*** | Tholeiite basalt | 746 | 0.9 | 9850 ± 300 | 2 |
| **Grímsvötn 9960 (G10ka Series #9)*** | Tholeiite basalt | 749 | 1 | 9960 ± 240 | 1 |
| **Grímsvötn 10120-10400 G10ka Series (1-8) (Tv-4)*** | Tholeiite basalt | 756-781 | 25 | 10120-10400 | 7 |
| Hekla 10550 | Alkali basalt | 802 | 0.3 | 10550 ± 150 | 2 |
| I-THOL-I? (Tv-3)* | Tholeiite basalt | 804 | 0.3 | 10560 ± 150 | 2 |
| Kverkfjöll 10630 | Tholeiite basalt | 812.5 | 0.3 | 10630 ± 150 | 3 |
| **Katla 11170** | Rhyolite, intermediate, alkali basalt | 827 | 0.4 | 11200 ± 330[2] | 3 |
| Katla 11295 | Rhyolite, intermediate, alkali basalt | 836 | 0.9 | 11360 ± 340 | 1 |
| **Katla 11315 (Tv-2)** | Rhyolite, intermediate, alkali basalt | 837 | 1.1 | 11375 ± 330[2] | 1 |
| **Hekla 11390 (Tv-1)** | Alkali basalt | 845 | 0.6 | 11390 ± 180[2] | 1 |

[1] Refers to depth in 2012NC sediment core.
[2] Ages reported in Harning et al. (2024).
[3] Indicates number of tephra fall events represented within individual tephra horizons. Total is 78.
*Established marker tephra layers from Iceland.
Bold ID indicates that residual sulfur content was measured in the groundmass glass of the tephra.
Underlined ID indicates potential regional markers.

## 3.2 Bulk geochemistry

Due to the high sampling density of bulk geochemistry ($n$ = 407) and BSi ($n$ = 284), the temporal resolution of Torfdalsvatn's record equates to an average of 1 sample every 27 and 39 years, respectively. Torfdalsvatn's magnetic susceptibility (MS) record shows the highest values at the base of the sediment core, which subsequently decrease to relatively low and stable values around 7000 cal a BP before rising again at 1350 cal a BP (Fig. 4a). %TOC ranges from 0.85 to 10.44 % with lowest values at the beginning of the record and highest values in the most recent portion, where a significant mean shift occurs at 8000 cal a BP (Fig. 4b). C/N values range from 5.33 to 11.13 with relatively high values from the beginning of the record to 7400 cal a BP, followed by a minimum between 7300 and 1080 cal a BP, before rising to reach a second maxima during the last several centuries (Fig. 4c). $\delta^{13}C$ values range from -23.05 to -15.87 ‰ and show large centennial-scale variability with the most $^{13}C$-depleted values occurring near the base and top of the record and are inversely related with C/N (Fig. 4d). Along with C/N values, $\delta^{13}C$ values are consistent with organic matter originating from a combination of aquatic and terrestrial sources, where their coincident changes (C/N increase and $^{13}C$-depletion) at 1800 cal a BP are consistent with a shift to a larger proportion of terrestrial organic matter to the lake (e.g., Geirsdóttir et al., 2020) (Fig. 4c-d). Finally, BSi ranges from 77 to 150 absorbance units, with the lowest values at the base and top of the record, and relatively higher but variable values in between (Fig. 4e). Although the discussion focuses on relative changes in %TOC and BSi, proxy fluxes are presented in the supporting information for reference (Fig. S5).

PCoA results for the bulk geochemistry proxy datasets show that axis 1 explains 52.4 % of the data's similarity (Fig. S6). PCoA axis 1 shows the highest values at the base of the record followed by a gradual decrease to a low at 7650 cal a BP (Fig. 4f). During the Middle Holocene, the PCoA values show some centennial scale variability, although millennial scale variability is relatively stable before a step shift at 1080 cal a BP (Fig. 4f). The major changes observed, such as the Early

Holocene decrease, Middle Holocene centennial-scale variability and step shift at 1080 cal a BP, coincide with either erosional

360   signals and/or tephra deposits (gray bars, Fig. 4). We therefore interpret PCoA axis 1 of bulk geochemistry to reflect relative changes in erosional activity.
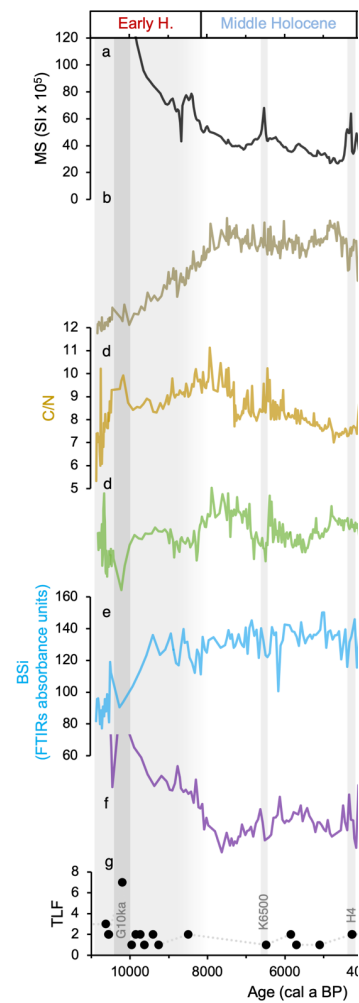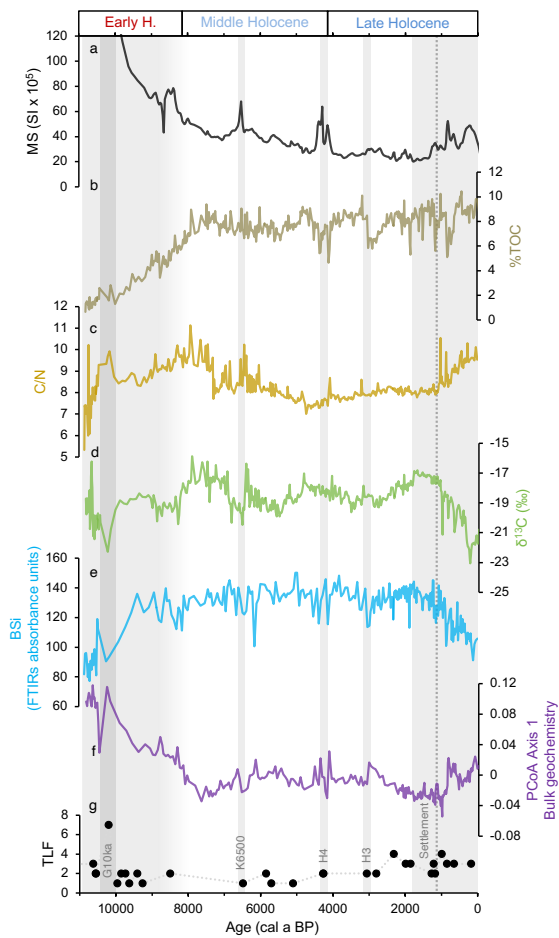
**Figure 4: Bulk physical and geochemical proxy records (a-e), PCoA Axis 1 of bulk geochemistry proxies (f), and tephra layer frequency (TLF, g) based on the number of events identified in each tephra layer (see Table 2) from core 2012NC. Note that MS in panel a is truncated at 120 SI x 10$^5$ and values at the base of the record reach up to 523 SI x 10$^5$. Grey bars reflect landscape disturbances associated with large tephra layer deposits and erosion and dashed gray line denotes the timing of presumed human settlement (1080 cal a BP).**

### 3.3 Algal pigments

The temporal resolution of Torfdalsvatn's algal pigment sampling ($n = 246$) equates to an average of 1 sample every 44 years. Algal pigment results are presented as the concentration of total chlorins (chlorophyll + degradation products pheophytin and pheophorbide), concentration of diatom pigments (fucoxanthin + diatoxanthin + diadinoxanthin), lutein to diatoxanthin ratio (L/D, ratio of green algae and higher plants to diatoms and chrysophytes, Leavitt and Hodgson, 2001), and the concentration of the cyanobacterial pigment canthaxanthin (Fig. 5). In all samples measured, chlorins are the most abundant pigments (Fig. 5a), making up between ~65 and 95 % of total pigments detected. In the earliest part of the record, chlorin concentrations are at their highest and rapidly decrease through 9450 cal a BP with a subsequent period of relatively elevated concentrations between 6030 and 3020 cal a BP (Fig. 5a). The proportion of diatom pigments is variable, ranging from ~1 to 27% of total pigment with the lowest relative abundance of diatom pigments occurring at the beginning of the record (Fig. 5b). After peaking at 8720 cal a BP, diatom pigment abundance begins to decrease, and along with inverse correlations with L/D, suggests that green algae became more abundant (Fig. 5b-c). Lutein-producing (green) species remain dominant, and the relative proportion of diatom pigments is low until 5560 cal a BP (Fig. 5b-c). Between 5560 and 1800 cal a BP, diatom pigments steadily increase, and L/D stays low (Fig. 5b-c), suggesting elevated diatom relative abundance through this interval before a change in sign in both proxies (low diatom pigments and increased L/D) during the last 1800 years. The only detectable pigment biomarker of cyanobacteria in Torfdalsvatn is canthaxanthin, present throughout the sediment core at low relative abundance between ~0.5 and 2.5% of total pigment (Fig. 5d). *Nostoc* sp. were commonly observed on shoreline rocks while sampling the epilithon in July 2014 and may therefore be a likely source of canthaxanthin. Except for the highest concentrations at the base of the record, cyanobacterial pigments are generally low until 8600 cal a BP, then steadily increase until 8040 cal a BP (Fig. 5d). Canthaxanthin concentrations remain high until ~5450 cal a BP, albeit with some variability, decreasing thereafter until reaching minimum values during the last 500 years (Fig. 5d). Post-depositional diagenesis does not appear to control any of the observed trends as pigment concentrations do not systematically decrease downcore and the highest concentrations are found in the oldest sediments. Although the discussion focuses on relative changes in pigments and their ratios, pigment fluxes are presented in the supporting information for reference (Fig. S5).

PCoA results for the algal pigment proxy datasets show that axis 1 explains 71 % of the data's similarity (Fig. S7). PCoA axis 1 closely resembles total diatom and chlorin pigments and shows relatively large centennial scale variability compared to the relatively stable millennial scale variability. Major deviations in the trends include a low from ~7250 cal a BP to 4950 cal a BP and a steady decline from 1800 cal a BP towards present (Fig. 5f). Given the strong similarity to algal pigment trends, we interpret PCoA axis 1 to reflect relative changes in total algal productivity.
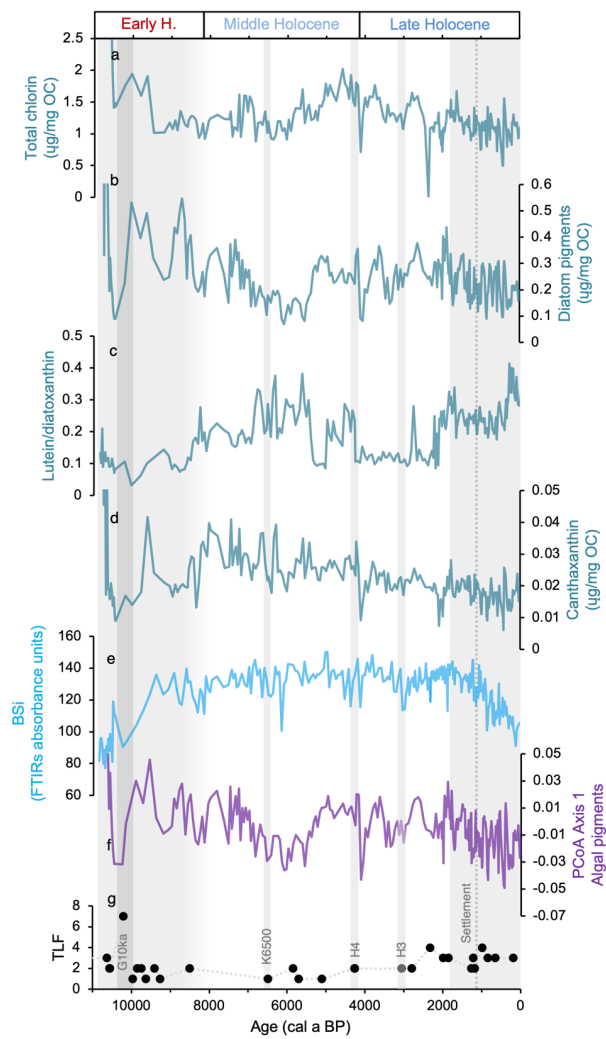
**Figure 5: Algal pigment proxy records (a-d), bulk geochemical BSi (e), PCoA Axis 1 of algal pigment proxies (f), and tephra layer frequency (TLF, g) based on the number of events identified in each tephra layer (see Table 2) from core 2012NC. Grey bars reflect landscape disturbances associated with large tephra layer deposits and erosion and dashed gray line denotes the timing of presumed human settlement (1080 cal a BP).**

## 4 Discussion

### 4.1 Holocene tephra records

Most lake sediment records in Iceland that report tephra compositional analyses only do so for key marker tephra to provide age control for accompanying proxy records. Currently, there are 5 regional lake record stratigraphies that provide complete tephra inventories for the sedimentary sequences (Fig. 6). Compared to these other detailed tephra stratigraphies, the 78 volcanic events identified in Torfdalsvatn are relatively extensive and only superseded by the lake Lögurinn record, which contains 149 volcanic events based on compositional analyses (Fig. 6, Gudmundsdóttir et al., 2016). Surprisingly, the tephra record from Hestvatn, which is located close to many of the active volcanic centers in south Iceland only archives 38 distinct volcanic events (Fig. 6, Geirsdóttir et al., 2022). The records from west (Haukadalsvatn) and northwest Iceland (Vestfirðir) contain 37 and 27 tephra layers, respectively (Harning et al., 2018, 2019). While various factors can influence the preservation of tephra layers in individual lake sediment records (e.g., Boygle, 1999), the simplest explanation for the regional variability in tephra layer occurrence is the direction of prevailing atmospheric winds around Iceland. In the stratosphere (7-15 km altitude), where explosive ash plumes are predominately injected to, the prevailing winds are westerly (Lacasse, 2001). However, if ash plumes are in the troposphere (<7 km altitude), upper stratosphere (>15 km altitude), or occur during the spring/summer when the prevailing stratospheric westerlies shift to weak easterlies (Lacasse, 2001), tephra can be carried westward.

In addition to the established Holocene tephra marker layers in the Icelandic record (highlighted with an * in Table 2), our high-resolution age model allows 14 additional tephra layers in Torfdalsvatn to serve as regional marker horizons in north Iceland. These include 1) the thick and closely-spaced Late Holocene basaltic Katla 1220 and Katla 1270 tephra layers, 2) the Middle Holocene sequence of Hekla 5100, Kverkfjöll/Katla 5850, Askja 6100 and Katla 6500 (Tv-5) series, 3) the Early Holocene Grímsvötn/Katla tephra pair G/K 8500 and Grímsvötn 9260, and 4) the pre-G10ka Series basaltic Hekla tephra layers, Hekla 10,550 and Hekla 11,390 (Tv-1), as well as the bimodal Katla tephra layers (Katla 11,170, Katla 11,295 and Katla 11,315, see Harning et al., 2024).

Finally, in this study, the residual sulfur content was measured in a selected suite of tephra samples (bold font, Table 2) to assess whether the events that produced those tephra layers involved interaction with external water upon eruption. Evidence of such interaction is an indicator of wet vent environment and thus may serve as a proxy for eruptions from within glaciers or through standing body of water (lake or the sea). We refer the reader to the Supporting Information for more details.

**Figure 6: Regional Icelandic tephra stratigraphies based on high-resolution lake sediment records from Hestvatn (Geirsdóttir et al., 2022), Haukadalsvatn (Harning et al., 2019), Vestfirðir (Harning et al., 2018), Torfdalsvatn (this study, Björck et al., 1992; Alsos et al., 2021; Harning et al., 2024), and Lögurinn (Gudmundsdóttir et al., 2016). For lake Lögurinn (east Iceland), we note that 149 total tephra layers have been identified and compositionally analyzed (Gudmundsdóttir et al., 2016), although we only show the key marker tephra layers for simplicity. All tephra layers are colored according to volcanic systems shown in Fig. 1a, and correlations between records indicated by dashed gray lines. Note: ages for tephra layers younger than the Settlement layer at ~1080 cal a BP (i.e., historical tephra) are presented in CE and not BP.**

## 4.2 Holocene climate and landscape evolution

Continuous records of past landscape stability and soil erosion can be reconstructed by comparing proxies for minerogenic flux (magnetic susceptibility, MS) and terrestrial versus aquatic organic matter source (C/N and $\delta^{13}C$) (e.g., Geirsdóttir et al., 2009, 2013, 2019, 2020). The controlling factors on the quantity of magnetic material that enters the lake are the amount of fine-grained minerogenic material available (from receding glaciers or tephra deposition), how well stabilized this material is

by vegetation, and the strength of a transport mechanism (erosion by wind or water). In Iceland, organic matter source can be distinguished as either terrestrial or aquatic via C/N and $\delta^{13}$C composition (Wang and Wooller, 2006; Skrzypek et al., 2008; Langdon et al., 2010; Florian, 2016), where terrestrial plants typically have high C/N (10 to 205) and low $\delta^{13}$C values (-31 to -22 ‰) and aquatic plants have relatively low C/N (7 to 26) and relatively high $\delta^{13}$C values (-30 to -11 ‰), with some overlap between end-members. Bulk sediment values therefore reflect the relative biomass in each environment, as well as efficiency of the transport of stored terrestrial material by soil erosion, which in Iceland, is easily accomplished by both wind and water due to the lack of cohesion of andosol soil (Arnalds, 2015). An increase in magnetic material (here inferred from magnetic susceptibility) without associated increase in C/N represents either an increase in available source material (such as tephra) or a relatively small carbon-producing biomass that reduces dilution of minerogenic material.

Biogenic silica (BSi), which reflects the relative amount of siliceous material produced by lake algae (mostly diatoms), is a commonly used measure for reconstructing total aquatic productivity (Conley and Schelske, 2001), and in Iceland, spring temperatures as well (Geirsdóttir et al., 2009). On the other hand, algal pigments provide a more comprehensive view of past aquatic productivity as they reflect other taxonomic groups, rather than just those that produce silicified structures (Leavitt and Hodgson, 2001), and primarily respond to broad changes in climate and nutrients (Smith, 1979; Smol and Cumming, 2000). Algal pigment concentrations and ratios, such as those presented here, can be used to characterize both total aquatic productivity and the relative contribution of major algal groups as most pigments used are relatively stable, reducing the bias of variable pigment preservation through time (Bianchi et al., 1993; Leavitt and Hodgson, 2001).

### 4.2.1 Deglaciation to Early Holocene (~12000 to 8200 cal a BP)

Based on the basal age of the Torfdalsvatn lake sediment core, deglaciation of this region of north Iceland is estimated to be around 12000 cal a BP (Harning et al., 2023). Subsequently, the receding Icelandic Ice Sheet left abundant, easily erodible minerogenic material upon the local landscape. Plant *sed*aDNA records from Torfdalsvatn indicate that the first pioneer forb, graminoid and bryophyte taxa were present in the catchment no earlier than 12,000 cal a BP (Fig. 7c, Alsos et al., 2021; Harning et al., 2024). The lack of a substantial terrestrial ecosystem needed to stabilize the landscape at this time is consistent with the highest MS values in Torfdalsvatn's Holocene record (Fig. 4a). MS then decreases as the quantity of easily erodible material was depleted and vegetation cover developed (Alsos et al., 2021). Woody taxa, such as *Salix* and *Betula*, then appear in the lake catchment by 10,300 and 9500 cal a BP, respectively (Alsos et al., 2021; Harning et al., 2023), straddling the deposition of the G10ka Series tephra and during the dominant period of terrestrial plant colonization (Alsos et al., 2021). MS values continue to steadily decrease through the G10ka Series tephra, although C/N increases, indicating a period of increased plant and soil erosion around Torfdalsvatn that has been previously associated with the massive amount of tephra fallout from the Grímsvötn eruptions (Rundgren, 1998; Hallsdóttir and Caseldine, 2005; Eddudóttir et al., 2015; Florian, 2016).

Throughout the Holocene record, chlorins are the most abundant algal pigment in Torfdalsvatn, consistent with their ubiquity in photosynthetic organisms and function as light-harvesting pigments (Simkin et al., 2022). In the Early Holocene, chlorin concentrations peak at 10760 cal a BP (Fig. 5a). At this time, significant terrestrial biomass had yet to develop on the

landscape (Alsos et al., 2021), meaning most organic matter was aquatic and algal pigment-rich, which is supported by low C/N and high $\delta^{13}$C values in bulk sediment (Fig. 4c-d). This is also consistent with a high proportion of unidentified *sed*aDNA reads, which is presumed to derive from algae due to limited reference material currently available (Alsos et al., 2021). The

605 subsequent decrease in chlorin concentrations (Fig. 5a) therefore likely reflects terrestrial biomass development (Alsos et al., 2021) and influx of algal pigment-poor material. This interpretation is supported by increasing C/N ratios, which indicate increased proportion of terrestrial carbon through this interval (Fig. 4c). The proportion of diagnostic pigments from algal groups (e.g., diatoms, L/D, and canthaxanthin) are variable during the Early Holocene. Diatom pigments become more abundant after the deposition of the G10ka Series tephra and an increase in BSi during this interval suggests an increase in

610 diatom productivity (Fig. 5b and e). These changes occur during a period of broad summer warming in Iceland, most clearly manifested in the rapid retreat and likely disappearance of residual Icelandic ice caps (Larsen et al., 2012; Harning et al., 2016b; Anderson et al., 2019). After peaking at 8720 cal a BP, diatom pigment concentrations decrease, inversely related with the ratio of lutein to diatoxanthin (Fig. 5b-c). This, along with a decrease in C/N (Fig. 4c), suggests that green algae and/or aquatic higher plants became more abundant at the expense of diatoms.

615 During the Early Holocene, marine sediment proxy records from the North Iceland Shelf indicate that surface currents were generally dominated by warm Atlantic Water and restricted sea ice (e.g., Kristjánsdóttir et al., 2017; Xiao et al., 2017; Harning et al., 2021) (Fig. 7). However, lake sediment and mire records from north Iceland document an interruption in woody taxa succession inferred from pollen and increased soil erosion from ~8800 to 7900 cal a BP (e.g., Hallsdóttir, 1995; Hallsdóttir and Caseldine, 2005; Eddudóttir et al., 2015, 2018; Geirsdóttir et al., 2020). This time window includes the well-known 8.2 ka

620 event (e.g., Barber et al., 1999; Alley and Ágústsdóttir, 2005; Rohling and Pälike, 2005) as well as additional freshwater pulses that originated from the decaying Laurentide Ice Sheet (e.g., Jennings et al., 2015) that are known to have driven oceanographic cooling around Iceland via a slowdown of the North Atlantic ocean circulation (e.g., Quillmann et al., 2012; Moossen et al., 2015). PCoA results for Torfdalsvatn soil erosion demonstrate that while the catchment was in transitional state towards stabilization (Fig. 7a), algal productivity generally decreases in response to cooling in the ~8800 to 7900 cal a BP window

625 (Fig. 7b). In terms of vegetation, plant *sed*aDNA species richness shows no change in woody, forbs, and bryophyte plant functional groups at this time, whereas others, such as graminoids and aquatic plants may have decreased. However, the low resolution of the *sed*aDNA record (>250 years, Fig. 7c) makes it challenging to confidently attribute changes to the ~8800 to 7900 cal a BP climate window specifically.

640
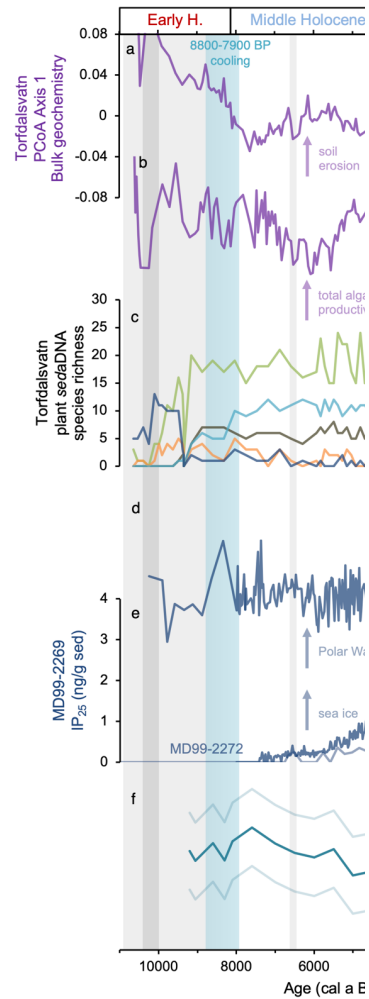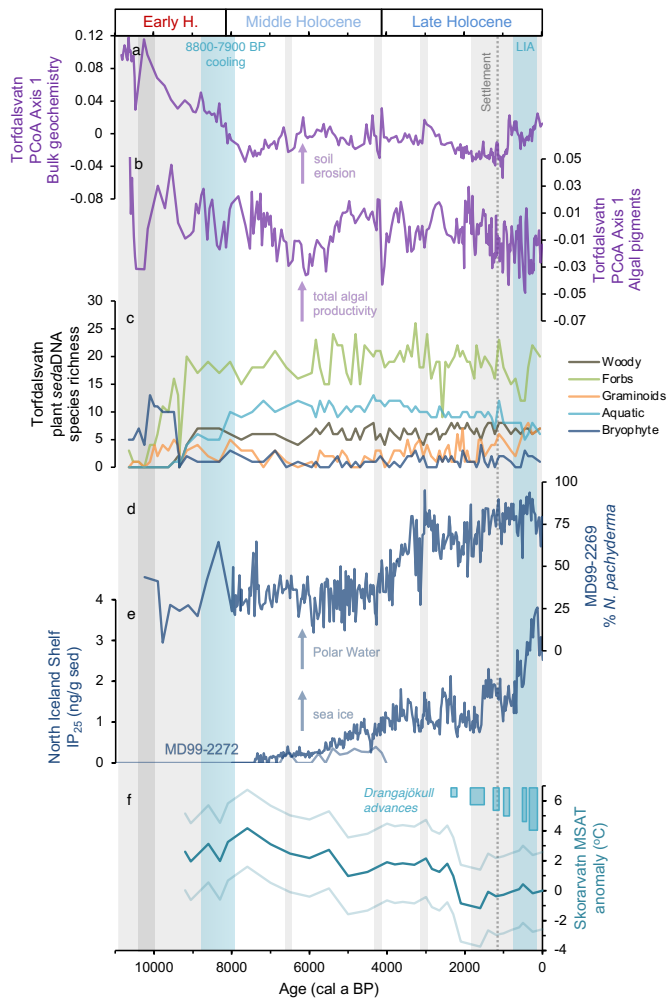
Figure 7: Comparison of Torfdalsvatn's PCoA results with regional marine and terrestrial environmental records. a) Torfdalsvatn PCoA Axis 1 of bulk geochemistry (this study), b) Torfdalsvatn PCoA Axis 1 of algal pigments (this study), c) Torfdalsvatn species richness of various plant functional groups based on *sed*aDNA (Alsos et al., 2021), d) relative abundance of Arctic planktic foraminifera *N. pachyderma* from marine core MD99-2269 (Harning et al., 2021), e) concentration of sea ice algae biomarker IP$_{25}$ from marine core MD99-2269 (dark blue, Cabedo-Sanz et al., 2016) and MD99-2272 (light blue, Xiao et al., 2017), and f) Drangajökull ice cap advances (blue, Harning et al., 2016a, 2018a) and mean summer air temperature anomaly (ºC) from Skorarvatn, NW Iceland (teal) with uncertainty estimates (light teal) (Harning et al., 2020). Grey bars reflect landscape disturbances associated with large tephra layer deposits and erosion and dashed gray line denotes the timing of presumed human settlement (1080 cal a BP).

### 4.2.2 Middle Holocene (8200 to 4200 cal a BP)

Overall, MS continues to decrease through the Middle Holocene, except for periodic spikes at 6500 and 4260 cal a BP reflecting the presence and impact of major tephra fall from Katla and Hekla eruptions, respectively (Fig. 4a). For the Katla 6500 tephra, increased C/N and δ$^{13}$C values indicate increased soil erosion immediately following its deposition, which lasted for several centuries (Fig. 4c-d). Similarly, Hekla 4 is known to have disturbed the terrestrial landscape in Icelandic lake catchments (Geirsdóttir et al., 2019), and in Torfdalsvatn, the period of increased erosion inferred from increased C/N and δ$^{13}$C values indicates that it only lasted for about a century (Fig. 4c-d). Eddudottir et al. (2017) suggest that lowland areas with presumably more substantial *Betula* woodland cover, such as Torfdalsvatn, are more resilient to tephra fall compared to higher elevation areas that were already at the climatic/ecological limit. The persistence of woody taxa around Torfdalsvatn through these large tephra fall events (Alsos et al., 2021) is consistent with this inference and suggests that the impact of periods of increased erosion were relatively shorter or less severe around Torfdalsvatn than they would otherwise be at higher elevation sites. However, we note that sampling resolution for *sed*aDNA in this portion of the record is over 100 years (Alsos et al., 2021), which may miss short-term impacts of tephra to the catchment ecosystem. In terms of aquatic proxies, we note that all algal pigments as well as BSi indicate short-lived increases in algal productivity during both the Katla 6500 and Hekla 4 eruptions. This process is consistent with lake studies in other volcanic regions that document increased diatom and algal productivity following volcanic eruptions due to the increased supply of silica and nutrients (e.g., Telford et al., 2004; Egan et al., 2019).

Chlorin concentrations remain generally low during the first two millennia of the Middle Holocene before increasing to peak values at 4580 cal a BP (Fig. 5a). These higher chlorin values are associated with increasing diatom pigments (Fig. 5b), decreasing L/D ratios (Fig. 5c), and the lowest C/N of the record (Fig. 4c), indicating a shift of organic matter towards a more aquatic plant source around this time. Interestingly, BSi does not track diatom pigment abundance for much of the record, which may be due to several complicating factors related to using both organic and inorganic indicators to reconstruct past algal biomass. Both proxies (i.e., diatom pigments and BSi) can be influenced by differences in amount of each compound per unit of algal biomass, varying species assemblage, and environmental conditions (Alberte et al., 1981; Lavaud et al., 2002; Rousseau et al., 2002; Stramski et al., 2002; Finkel et al., 2010), all of which are challenging to individually constrain in paleoenvironmental reconstructions. In any case, during the Middle Holocene, terrestrial pollen (Rundgren, 1998; Hallsdóttir

Deleted: At least f

Deleted: has

Deleted: similarly

Deleted: other

Deleted: , however,

Deleted:

Deleted:

Deleted: . One possibility is that there are

Deleted: these

and Caseldine, 2005; Eddudóttir et al., 2015) and plant *sed*aDNA records (Alsos et al., 2021) indicate that catchment vegetation communities were well-developed, which likely stabilized the catchment and reduced the influx of terrestrial organic matter to the lake. In addition, aquatic plants make up the dominant proportion of *sed*aDNA reads at this time (Alsos et al., 2021), which likely results from the small, shallow nature of the lake basin that permits light penetration for submerged taxa (Fig 1b), consistent with the increased general productivity of the aquatic environment.

Finally, cyanobacterial populations have been shown to quickly increase in response to higher temperature and nutrient levels and may therefore be an important indicator species for past lake conditions (De Senerpont Domis et al., 2007; Paerl and Paul, 2012). The only detectable pigment of cyanobacteria in Torfdalsvatn is canthaxanthin, present throughout the core at low concentrations. Canthaxanthin concentrations remain elevated until ~5450 cal a BP, albeit with some variability, decreasing thereafter until reaching minimum values during the last 500 years (Fig. 5d). The pattern of change in canthaxanthin concentrations mirrors other relative and quantitative temperature records derived from Icelandic lake sediment BSi composites and lipid biomarkers records, respectively, which peak during the Holocene Thermal Maximum (7900 to 5500 cal a BP) and decrease in a stepwise manner through the Middle Holocene to the Little Ice Age (700 to 50 cal a BP, 1250 to 1900 CE) (Larsen et al., 2012; Geirsdóttir et al., 2013, 2019, 2020; Harning et al., 2020). This suggests that the abundance of cyanobacteria may be controlled more closely by lake water temperature and length of summer than the other algal groups in Torfdalsvatn, such as diatoms.

PCoA results from bulk geochemistry and plant *sed*aDNA species richness demonstrate that the Middle Holocene terrestrial landscape around Torfdalsvatn was generally stable, whereas algal productivity diminished between 7500 and 5000 cal a BP (Fig 7a-c). This terrestrial stability is consistent with the corresponding marine environment along the North Iceland Shelf, where the ocean surface was dominated by warm Atlantic Water at this time (e.g., Kristjánsdóttir et al., 2017; Harning et al., 2021), reflected well by low abundances of Arctic planktic foraminifera (e.g., *N. pachyderma*, Harning et al., 2021) and sea ice algae proxies (e.g., IP$_{25}$, Cabedo-Sanz et al., 2016; Xiao et al., 2017) (Fig. 7d-e). The decrease in algal productivity between 7500 and 5000 cal a BP in the PCoA results largely stems from decreases in diatom pigments as well as minor decreases in chlorins at the expense of lutein-producing green algae and/or higher plants (Fig. 5). As there is no indication of local climate change during the 7500 to 5000 cal a BP interval in either the Icelandic marine or terrestrial realms, it is possible that the changes resulted from internal lake dynamics, such as nutrient availability. However, without further proxy information, the processes behind the changes in algal productivity are currently challenging to diagnose.

**4.2.3 Late Holocene (4200 cal a BP to present)**

After about two millennia of relative stability in Torfdalsvatn following the Hekla 4 tephra layer, individual algal pigment concentrations, BSi, and algal pigment PCoA results begin to decrease at 1800 cal a BP (150 CE, Fig. 5). These consistent changes indicate broad decreases in total algal productivity likely driven by ambient changes in climate and/or shorter ice-free seasons that inhibit light availability. However, we do not find an increase in C/N or soil erosion accompanying algal productivity changes around Torfdalsvatn, similar to other high-resolution lake sediment proxy records in Iceland (e.g.,

| Deleted: logical |
| Deleted: were induced by |
| Deleted: processes |

| Deleted: In contrast to other high resolution lake sediment C/N proxy records in Iceland (Geirsdóttir et al., 2019, 2020) |
| Deleted: . |

Geirsdóttir et al., 2013, 2019, 2020). This is consistent with the low elevation and low relief nature of Torfdalsvatn's catchment and relative stability of the various terrestrial plant functional groups in the lake catchment derived from *sed*aDNA (Fig. 7C, Alsos et al., 2021). However, regime shifts in offshore marine climate records demonstrate that around this time (i.e., ~1800 cal a BP, 150 CE) the Polar Front advanced southward around Iceland, bathing the North Iceland Shelf with cool, sea-ice bearing Polar Water (Harning et al., 2021). This shift in ocean surface water source is reflected well by the increase in Arctic

730     planktic foraminifera *N. pachyderma* (Harning et al., 2021) and sea ice algae proxy IP$_{25}$ (Cabedo-Sanz et al., 2016) from sediment cores on the North Iceland Shelf just north of Torfdalsvatn (MD99-2269, Figs. 1A and 7d-e), and led to substantial summer cooling in the area around Skorarvatn, NW Iceland, resulting in the marginal expansion of the nearby Drangajökull ice cap, just west of Torfdalsvatn (Figs. 1a and 7f, Harning et al., 2016a, 2018a, 2020).

735     At 880 cal a BP (1070 CE), bulk geochemistry PCoA results indicate a substantial increase in landscape instability and soil erosion around Torfdalsvatn (Fig. 7a). Norse settlers are estimated to have arrived in Iceland earlier, i.e., around 1080 cal a BP (870 CE), and *assumed* to have quickly impacted the landscape through woodland clearing and agricultural and pastoral farming that prohibited natural plant regeneration (e.g., Thórarinsson, 1944; Arnalds, 1987; Hallsdóttir, 1987; Smith, 1995; Lawson et al., 2007). However, these datasets are largely based on soil and sedimentary records with coarser resolution

740     and/or age control than Torfdalsvatn. For Torfdalsvatn, the earliest known presence of humans around the lake is later than both the geochemical record and assumed settlement in 665 cal a BP (1285 CE), when the local farms sharing the lake are mentioned in a letter as being owned by the Þingeyrarklaustur monastery (DI, 1857-1986). The plant *sed*aDNA record from Torfdalsvatn indicates that while some woody taxa, such as *Salix* and *Betula*, are present through the presumed timing of human colonization around 1080 cal a BP (870 CE), *J. communis* (juniper) disappears and species diversity of forbs decrease

745     slightly earlier than our bulk geochemistry record and documentary evidence of human presence (1055 cal a BP, 895 CE, Fig. 7C, Alsos et al., 2021). We note, however, that while environmental impacts from settlers have been independently confirmed in lake sediments on the Faroe and Lofoten Islands using fecal biomarkers and/or sheep *sed*aDNA (D'Anjou et al., 2012; Curtin et al., 2021), these tools have so far proved challenging for use in Icelandic sediments and are needed for confirmation (Ardenghi et al., 2024). Hence, it is difficult to correlate whether the changes in soil erosion around Torfdalsvatn are related

750     to human pressure or otherwise. In any case, it is unlikely that the small populations that initially settled Iceland (~30,000 people, *Landnámabók*, i.e. The book of Settlement) would have had a substantial and immediate impact on the landscape. If we can independently confirm human presence in Torfdalsvatn sedimentary record through future application of molecular approaches, such as fecal biomarkers and mammalian *sed*aDNA, our record from Torfdalsvatn will provide a well-constrained benchmark for changes in the ecosystem linked to human practices in north Iceland.

755     Following the initiation of increased long-term soil erosion that began around 880 cal a BP, we observe distinct disturbances to the Hekla 1104 CE (846 cal a BP) tephra layer stratigraphy. In core 2004NC, Hekla 1104 CE tephra is present over a 15.4 cm interval (88.1 to 103.5 cm depth) as three distinct and separate layers/wedges connected by mm-thick, irregular light-colored stringers with intermittent shear planes (Fig. 8). The 30 cm above the uppermost wedge is characterized by fining upward pumice grains suggesting an origin within a gravity current (Fig. 8). In core 2012NC, it is present as two distinct layers

Deleted: and

Deleted: s

Deleted: this interval

Deleted: , which may partially be due to variable age control between the two sedimentary records

Deleted: , and

Deleted: s

Deleted: 10

at depths of 80.5 cm (0.1 cm) and 84.5 cm (0.7 cm) (see Supporting Information), where the upper layer has a modeled age of 800 cal a BP (1150 CE). Hekla 1104 CE is also found in a previously published record from Torfdalsvatn (Alsos et al., 2021),

770 where the stratigraphy is also discontinuous with stringers below and above the main tephra layer horizon (Bender, 2020). The cause of this disturbance is unlikely to relate to sediment coring as it is found in the middle of the core segments between undisturbed organic lake sediment and identified in three independent records. Instead, this indicates that an external factor likely impacted the sedimentary sequence after the Hekla 1104 CE tephra layer was deposited, such as a slope failure. As the catchment and bathymetry of Torfdalsvatn are both low relief (Fig. 1b, Florian, 2016), a slope failure would require a trigger

775 event. Local documentary records indicate that a large earthquake occurred in 1260 CE (Storm, 1977a, 1977b, 1977c), which we propose as a likely candidate based on the slightly younger age compared to the tephra deposit. Similar soft sediment deformation structures in tephra layers have been identified in New Zealand lakes and linked to seismic activity (termed tephra-seismites, Kluger et al., 2023), supporting our reasoning for Torfdalsvatn's stratigraphy. While the disturbance is relatively short-lived, the Torfdalsvatn records indicate the susceptibility of even low-relief environments to seismic activity that may

780 confound the continuity and interpretation of lake sediment proxies in Iceland.
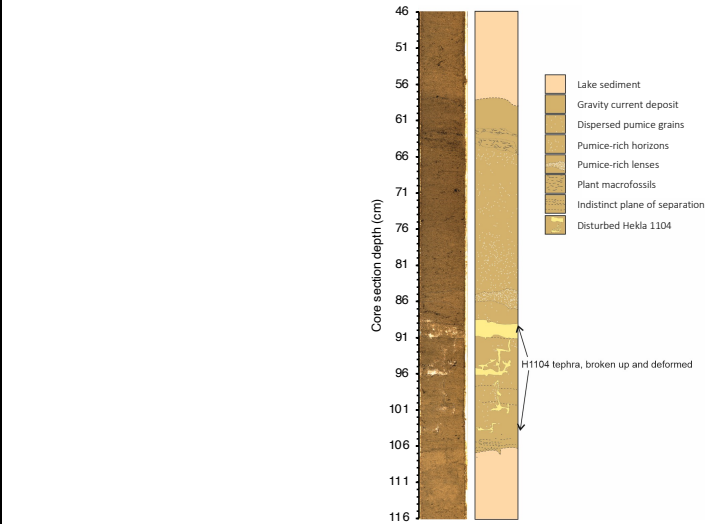
**Figure 8: Lithostratigraphy of the deformed Hekla 1104 CE tephra layer (i.e., tephra-seismite) in core 2004NC. On the left is a photo image and on the right is a simplified schematic based on the major identified sediment types.**
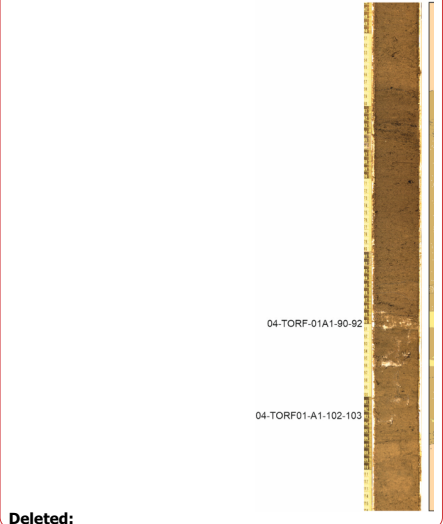
Finally, the general cooling reflected in decreased algal productivity that commenced at 1800 cal a BP (150 CE) culminated with the lowest Late Holocene values at 450 cal a BP (1500 CE, Fig. 7b). This coincides with the Little Ice Age (LIA, ~700 to 100 cal a BP, 1250 to 1850 CE, blue bar, Fig. 7, Geirsdóttir et al., 2013), a period marked by the coolest Holocene

790 conditions in Iceland. Regionally, the Little Ice Age is well reflected in environmental conditions such as the maximum Holocene extent of Polar Water and sea ice on the North Iceland Shelf (Fig. 7d-e, Cabedo-Sanz et al., 2016; Harning et al., 2021) and largest Holocene dimensions of Icelandic ice caps (Fig. 7f, Larsen et al., 2011; Harning et al., 2016b; Hannesdóttir et al., 2015, 2020). In terms of Torfdalsvatn plant communities, species richness patterns show troughs in forbs and aquatic taxa and peaks in graminoids and bryophytes during this interval (Fig. 7c). Alsos et al. (2021) also note an increase of high

795 arctic taxa such as *O. digyna*, *K. islandica*, *Epilobium anagallidifolium*, *S. acaulis*, and *D. octopetala* at Torfdalsvatn during the Little Ice Age. Despite these broad changes in Torfdalsvatn's terrestrial and aquatic environments during the coldest part of the Holocene – that would be expected to result in enhanced landscape instability as observed in other Icelandic lake records (e.g., Geirsdóttir et al., 2009, 2020) – we observe a decrease in soil erosion between 650 and 100 cal a BP (1300 to 1850 CE, Fig. 7a). The northern latitudinal position of the lake abutting the harsh Polar marine climate on the North Iceland Shelf and

800 minima in Northern Hemisphere summer insolation (Berger and Loutre, 1991) would have resulted in shorter summers and possibly reduced mobilization of soil in a more perennially frozen landscape, and therefore explain a decrease in soil erosion. Following the termination of the Little Ice Age (100 cal a BP, 1850 CE), the Torfdalsvatn record indicates a slight decrease in soil erosion and algal productivity to present (Fig. 7a-b). While it is challenging to directly tie this period to Iceland's instrumental temperature record because 1) we lack secure chronological control from the last century (e.g., ^{137}Cs) and 2) this

805 period is only represented by several data points, these proxy trends suggest that the broad warming trend that followed the end of the Little Ice Age (Hanna et al., 2004) may have resulted in reduced soil erosion and algal productivity. However, with the concomitant rise in Iceland's population (Hagstofa Íslands, 2024), increased human pressure may have also impacted the landscape. Future higher-resolution studies focusing on the last several centuries in Icelandic lakes will be instrumental in deciphering the most recent changes in the environment and how that relates to human and climate drivers.

810 **5 Conclusions**

We present a multi-proxy analysis of lake sediments from Torfdalsvatn, the longest known lacustrine record in Iceland of ~12000 years. These analyses include a detailed age model (*n* = 20 control points), an expanded and comprehensive Holocene tephra stratigraphy and chronology (>2200 grains analyzed in 33 tephra horizons), and sub-centennial bulk geochemical and algal pigment proxy records. Collectively, we use these datasets to address the following topics:

815 • *Tephrochronology:* We identified 33 distinct tephra layers, which represent 78 separate volcanic events from 6 volcanic systems. Compared to tephra stratigraphies from other lake sediment records in Iceland, these are relatively high numbers. Key marker tephra layers include I-THOL-I, the G10ka Series (13 events), Katla 6500, Hekla 4, Hekla 3, Hekla C, Hekla 1104, Hekla 1300, and Hekla 1766. In addition, we present evidence for a previously unidentified

basalt tephra (Askja 6100) with a distinct primitive composition and a bimodal (rhyolite-basalt) tephra layer (Hekla
825     5100).

- *Catchment instability and soil erosion:* Bulk physical and geochemical proxy records capture past intervals of soil erosion around Torfdalsvatn due to combinations of Middle Holocene volcanic eruptions, Late Holocene climate cooling and after presumed human settlement at 880 cal a BP (1070 CE). Compared to other lake sediment records in Iceland, we do not observe clear long-term increases in soil erosion beginning prior to human settlement but starting ~200 years later. The stratigraphy (i.e., tephra-seismite) of sediment during the last millennium also suggests the occurrence of a seismic-induced slope failure in or around the lake.

- *Algal productivity:* Torfdalsvatn's algal group ontogeny progressed from mainly diatoms shortly after the G10ka Series tephra, to predominantly green algae, aquatic macrophytes and cyanobacteria. This is assumed to have been driven by increased temperatures and length of summer during the HTM where the timing of peak cyanobacterial abundance likely represents the warmest Holocene temperatures in Torfdalsvatn. After the HTM, algal productivity remains generally stable until 1800 cal a BP, when changes in regional climate led to decreased algal productivity that reached the lowest values during the Little Ice Age (700 to 100 cal a BP, 1250 to 1850 CE).

- The changes in algal productivity and soil erosion observed beginning around 1800 (150 CE) and 880 cal a BP (1070 CE), respectively, highlight the impact of both natural and possibly anthropogenic factors on Late Holocene aquatic and terrestrial environmental changes in north Iceland. Importantly, they emphasize that while local climate was cooling prior to known human settlement, some low-elevation coastal regions such as Torfdalsvatn, may have been more resistant to natural pre-settlement changes in vegetation cover and soil erosion than observed in other regions of Iceland.

**Data Availability**

845  Data associated with this manuscript is available in the Supporting Information and at the NOAA NCEI Paleoclimatology database (https://www.ncei.noaa.gov/access/paleo-search/study/39580).

**Author Contributions**

ÁG and GHM conceptualized and funded the research; ÁG, GHM, CRF and YA acquired lake sediment cores; SÓ performed PSV analyses; DJH and TT performed EMP analyses and generated the age model; CRF analyzed bulk geochemistry and algal
850  pigments; DJH, CRF, ÁG and TT wrote the paper with contribution from all co-authors.

**Competing Interests**

The authors declare that they have no conflict of interest.

**Acknowledgements**

855 We kindly thank Guðrún Eva Jóhannsdóttir for her contribution to electron microprobe measurements and Þorsteinn Jónsson, Sveinbjörn Steinþórsson, Jason Briner, Yiming Wang, and Matt Wooller for assistance in the field. CRF acknowledges support from the Doctoral Grant of the University of Iceland. This project has been principally supported by the Icelandic Center for Research (RANNÍS) through Grant-of-Excellences #022160002-04, #70272011-13 and #141573051-3, the University of Iceland Research Fund, and the National Science Foundation ARCSS #1836981, awarded to ÁG and GHM.

860

**References**

Abbott, P. M., and Davies, S. M.: Volcanism and the Greenland ice-cores: the tephra record, Earth-Science Reviews, 115, 173-191, https://doi.org/10.1016/j.earscirev.2012.09.001, 2012.

Alberte, R. S., Friedman, A. L., Gustafson, D. L., Rudnick, M. S., and Lyman, H.: Light-harvesting systems of brown algae
865 and diatoms. Isolation and characterization of chlorophyll a c and chlorophyll a fucoxanthin pigment-protein complexes, Biochimica et Biophysica Acta (BBA) - Bioenergetics, 635, 304–316, https://doi.org/10.1016/0005-2728(81)90029-3, 1981.

Alley, R., and Ágústsdóttir, A.: The 8k event: Cause and consequences of a major Holocene abrupt climate change, Quaternary Science Reviews, 24, 1123-1149, https://doi.org/10.1016/j.quascirev.2004.12.004, 2005.

870 Alsos, I. G., Lammers, Y., Kjellman, S. E., Merkel, M. K. F., Bender, E. M., Rouillard, A., Erlendsson, E., Guðmundsdóttir, E. R., Benediktsson, I. Ö., Farnsworth, W. F., Brynjólfsson, S., Gísladóttir, G., Eddudóttir, S. D., and Schomacker A.: Ancient sedimentary DNA shows rapid post-glacial colonisation of Iceland followed by relatively stable vegetation until the Norse settlement (Landnám) AD 870, Quaternary Science Reviews, 259, 106903, https://doi.org/10.1016/j.quascirev.2021.106903, 2021.

875 Anderson, L. S., Flowers, G. E., Jarosch, A. H., Aðalgeirsdóttir, G. Th., Geirsdóttir, Á., Miller, G. H., Harning, D. J., Thorsteinsson, T., Magnússon, E., and Pálsson, F.: Holocene glacier and climate variations in Vestfirðir, Iceland, from the modeling of Drangajökull ice cap, Quaternary Science Reviews, 190, 39-56, https://doi.org/10.1016/j.quascirev.2018.04.024, 2018.

880 Anderson, L. S., Geirsdóttir, Á., Flowers, G. E., Wickert, A. D., Aðalgeirsdóttir, G. Th., and Thorsteinsson, T.: Controls on the lifespans of Icelandic ice caps, Earth and Planetary Science Letters, 527, 115780, https://doi.org/10.1016/j.epsl.2019.115780, 2019.

885   Ardenghi, N., Harning, D. J., Raberg, J. H., Holman, B. R., Thordarson, T., Geirsdóttir, Á., Miller, G. H., Sepúlveda, J.: A Holocene history of climate, fire, landscape evolution, and human activity in Northeast Iceland, Climate of the Past, in press, https://doi.org/10.5194/cp-2023-74, 2024.

Arnalds, A.: Ecosystem disturbance in Iceland, Arctic and Alpine Research, 19, 508-513, https://doi.org/10.2307/1551417,
890   1987.

Arnalds, O.: The Soils of Iceland. Springer, 2015.

Arnalds, O., and Gretarsson, E.: Soil map of Iceland. Agricultural Research Institute, Reykjavík, 2021.

895   Arnolds, Ó., Marteinsdóttir, B., Brink, S.H., and Órsson, J.: A framework model for current land condition in Iceland, PloS ONE, 18, e0287764, https://doi.org/10.1371/journal.pone.0287764, 2023.

Axford, Y., Geirsdóttir, Á., Miller, G. H., and Langdon, P.: Climate of the Little Ice Age and the past 2000 years in northeast Iceland inferred from chironomids and other lake sediment proxies, Journal of Paleolimnology, 41, 7-24, https://doi.org/10.1007/s10933-008-9251-1, 2009.
900

Axford, Y., Miller, G. H., Geirsdóttir, Á., and Langdon, P.: Holocene temperature history of northern Iceland inferred from subfossil midges, Quaternary Science Reviews, 26, 3344-3358, https://doi.org/10.1016/j.quascirev.2007.09.003, 2007.

Bates, R., Erlendsson, E., Eddudóttir, S. D., Möckel, S. C., Tinganelli, L., and Gísladóttir, G.: *Landnám*, land use and landscape change in Kagaðarhóll in Northwest Iceland, Environmental Archaeology, 27, 211-227,
905   https://doi.org/10.1080/14614103.2021.1949680, 2021.

Barber, D. C., Dyke, A., Hillaire-Marcel, C., Jennings, A. E., Andrews, J. T., Kerwin, M. W., Bilodeau, G., McNeely, R., Southon, J., Morehead, M. D., and Gagnon, J. M.: Forcing of the cold event of 8,200 years ago by catastrophic drainage of Laurentide lakes, Nature, 400, 344-348, https://doi.org/10.1038/22504, 1999.

910   Bender, E. M.: Late Quaternary tephra stratigraphy and paleoenvironmental reconstruction based on lake sediments from North and Northeast Iceland, MS thesis, UiT The Arctic University of Norway, 2020.

Berger, A., and Loutre, M. F.: Insolation values for the climate of the last 10 million years, Quaternary Science Reviews, 10, 297-317, https://doi.org/10.1016/0277-3791(91)90033-Q, 1991.
915

Bergman, J., Wastegård, S., Hammarlund, D., Wohlfarth, B., and Roberts, S. J.: Holocene tephra horizons at Klocka Bog, west-central Sweden: aspects of reproducibility in subarctic peat deposits, Journal of Quaternary Science, 19, 241-249, https://doi.org/10.1002/jqs.833, 2004.

920     Bianchi, T. S., Dibb, J. E., and Findlay, S.: Early diagenesis of plant pigments in Hudson River sediments, Estuarine, Coastal and Shelf Science, 36, 517–527, https://doi.org/10.1006/ecss.1993.1031, 1993.

Birks, H. H., Gulliksen, S., Haflidason, H., Mangerud, J., and Possnert, G.: New radio-carbon dates from the Vedde ash and Saksunarvatn ash western Norway, Quaternary Research, 127, 119-127, https://doi.org/10.1006/qres.1996.0014, 1996.

925

Björck, S., Ingólfsson, Ó., Haflidason, H., Hallsdóttir, M., and Anderson, N. J.: Lake Torfadalsvatn: a high resolution record of the North Atlantic ash zone I and the last glacial-interglacial environmental changes in Iceland, Boreas, 21, 15-22, https://doi.org/10.1111/j.1502-3885.1992.tb00009.x, 1992.

930     Blaauw, M., and Christen, J. A.: Flexible paleoclimate age-depth models using an autoregressive gamma process, Bayesian Analysis, 6, 457–474, http://doi.org/10.1214/11-BA618, 2011.

Blaauw, M., Christen, J. A., Bennett, K. D., and Reimer, P. J.: Double the dates and go for Bayes – Impacts of model choice, dating density and quality on chronologies, Quaternary Science Reviews, 188, 58-66,
935     https://doi.org/10.1016/j.quascirev.2018.03.032, 2018.

Blair, C. L., Geirsdóttir, Á., and Miller, G. H.: A high-resolution multi-proxy lake record of Holocene environmental change in southern Iceland, Journal of Quaternary Science, 30, 281-292, https://doi.org/10.1002/jqs.2780, 2015.

940     Boygle, J.: Variability of tephra in lake and catchment sediments, Svínavatn, Iceland, Global and Planetary Change, 21, 129-149, https://doi.org/10.1016/S0921-8181(99)00011-9, 1999.

Bradley, L.-A. and Stafford, T. W.: Comparison of manual and automated pretreatment methods for AMS radiocarbon dating of plant fossils, Radiocarbon, 36, 399–405, https://doi.org/10.1017/S0033822200014570, 1994.
945

Bronk Ramsey, C.: Bayesian analysis of radiocarbon dates, Radiocarbon, 51, 337-360, https://doi.org/10.1017/S0033822200033865, 2009.

Cabedo-Sanz, P., Belt, S. T., Jennings, A. E., Andrews, J. T., and Geirsdóttir, Á.: Variability in drift ice export from the Arctic Ocean to the North Icelandic Shelf over the last 8000 years: A multi-proxy evaluation, Quaternary Science Reviews, 146, 99–115, https://doi.org/10.1016/j.quascirev.2016.06.012, 2016.

Caseldine, C., Geirsdóttir, Á., and Langdon, P. G.: Efstadalsvatn – a multi-proxy study of a Holocene lacustrine sequence from NW Iceland, Journal of Paleolimnology, 30, 55-73, https://doi.org/10.1023/A:1024781918181, 2003.

Caseldine, C., Langdon, P., and Holmes, N.: Early Holocene climate variability and the timing and extent of the Holocene thermal maximum (HTM) in northern Iceland, Quaternary Science Reviews, 25, 2314-2331, https://doi.org/10.1016/j.quascirev.2006.02.003, 2006.

Conley D. J. and Schelske, C. L.: Biogenic Silica. Track Environmental Change Using Lake Sediments 3, 281–293, 2001.

Curtin, L., D'Andrea, W. J., Balascio, N. L., Shirazi, S., Shapiro, B., de Wet, G. A., and Bradley, R. S., Bakke, J.: Sedimentary DNA and molecular evidence for early human occupation of the Faroe Islands, Communications Earth & Environment, 2, 253, https://doi.org/10.1038/s43247-021-00318-0, 2021.

D'Anjou, R. M., Bradley, R. S., Balascio, N. L., and Finkelstein, D. B.: Climate impacts on human settlement and agricultural activities in northern Norway revealed through sediment biogeochemistry, Proceedings of the National Academy of Sciences, 109, 20332–20337, https://doi.org/10.1073/pnas.1212730109, 2012.

Davies, S. M., Albert, P. G., Bourne, A. J., Owen, S., Svensson, A., Bolton, M. S. M., Cook, E., Jensen, B. J. L., Jones, G., Ponomareva, V. V., and Suzuki, T.: Exploiting the Greenland volcanic ash repository to date caldera-forming eruptions and widespread isochrons during the Holocene, Quaternary Science Reviews, 334, 108707.

De Senerpont Domis, L. N., Mooij, W. M., and Huisman, J.: Climate-induced shifts in an experimental phytoplankton community: A mechanistic approach, Hydrobiologia, 584, 403–413, https://doi.org/10.1007/s10750-007-0609-6, 2007.

DI Diplomatarium Islandicum): Íslenzkt Fornbréfasafn III. Íslenzka Bókmenntafélagið, Kaupmannahöfn (Copenhagen), 1857-1986.

Dugmore, A. J., and Buckland, P. C.: Tephrochronology and late Holocene soil erosion in south Iceland. In: Maizels, Judith K., Caseldine, Christopher (Eds.), Environmental Change in Iceland Past and Present. Dordrecht, the Netherlands: Kluwer, pp. 147-161, 1991.

Dugmore, A. J., and Erskine, C. C.: Local and regional patterns of soil erosion in southern Iceland, Münchener Geographische Abhandlungen, 2, 63-79, 1994.

980

Dugmore, A. J., Cook, G. T., Shore, J. S., Newton, A. J., Edwards, K. J., and Larsen, G.: Radiocarbon dating tephra layers from Britain and Iceland, Radiocarbon, 37, 379-388, https://doi.org/10.1017/S003382220003085X, 1995.

Eddudóttir, S. D., Erlendsson, E., and Gísladóttir, G.: Life on the periphery is tough: Vegetation in Northwest Iceland and its

985   responses to early-Holocene warmth and later climate fluctuations, The Holocene, 25, 1437-1453, https://doi.org/10.1177/0959683615585839, 2015.

Eddudóttir, S. D., Erlendsson, E., and Gísladóttir, G.: Effects of the Hekla 4 tephra on vegetation in northwest Iceland, Vegetation History and Archaeobotany, 26, 389-402, https://doi.org/10.1007/s00334-017-0603-5, 2017.

990

Eddudóttir, S.D., Erlendsson, E., Gísladóttir, G.: An Icelandic terrestrial record of North Atlantic cooling c. 8800-8100 cal. yr BP, Quaternary Science Reviews, 197, 246-256, https://doi.org/10.1016/j.quascirev.2018.07.017, 2018.

Eddudóttir, S. D., Erlendsson, E., Tinganelli, L., and Gísladóttir, G.: Climate change and human impact in a sensitive

995   ecosystem: the Holocene environment of the Northwest Icelandic highland margin, Boreas, 45, 715-728, https://doi.org/10.1111/bor.12184, 2016.

Egan, J., Allott, T. E. H., and Blackford, J. J.: Diatom-inferred aquatic impacts of the mid-Holocene eruption of Mount Mazama, Oregon, USA, Quaternary Research, 91, 163-178, https://doi.org/10.1017/qua.2018.73, 2019.

1000  Finkel, Z. V., Matheson, K. A., Regan, K. S., and Irwin, A. J.: Genotypic and phenotypic variation in diatom silicification under paleo-oceanographic conditions, Geobiology, 8, 433–445, https://doi.org/10.1111/j.1472-4669.2010.00250.x, 2010.

Fisher, R. V., and Schmincke, H.-U.: Pyroclastic Rocks. Springer Verlag, Berlin-Heidelberg, 472 pages, 1984.

Florian, C. R.: Multi-proxy Reconstructions of Holocene Environmental Change and Catchment Biogeochemistry Using Algal

1005  Pigments and Stable Isotopes Preserved in Lake Sediment from Baffin Island and Iceland. PhD thesis, University of Colorado Boulder and University of Iceland, 2016.

Flowers, G. E., Björnsson, H., Geirsdóttir, Á., Miller, G. H., Black, J. L., and Clarke, G. K. C.: Holocene climate conditions and glacier variation in central Iceland from physical modelling and empirical evidence, Quaternary Science Reviews, 27, 797-813, https://doi.org/10.1016/j.quascirev.2007.12.004, 2008.

Gathorne-Hardy, F. J., Erlendsson, E., Langdon, P. G., and Edwards, K. J.: Lake sediment evidence for late Holocene climate change and landscape erosion in western Iceland, Journal of Paleolimnology, 42, 413-426, https://doi.org/10.1007/s10933-008-9285-4, 2009.

Geirsdóttir, Á., Harning, D. J., Miller, G. H., Andrews, J. T., Zhong, Y., and Caseldine, C.: Holocene history of landscape instability in Iceland: Can we deconvolve the impacts of climate, volcanism and human activity?, Quaternary Science Reviews, 249, 106633, https://doi.org/10.1016/j.quascirev.2020.106633, 2020.

Geirsdóttir, Á., Miller, G. H., Andrews, J. T., Harning, D. J., Anderson, L. S., Florian, C., Larsen, D. J., and Thordarson, T.: The onset of Neoglaciation in Iceland and the 4.2 ka event, Climate of the Past, 15, 25-40, https://doi.org/10.5194/cp-15-25-2019, 2019.

Geirsdóttir, Á., Miller, G. H., Harning, D. J., Hannesdóttir, H., Thordarson, T., and Jónsdóttir, I.: Evidence for recurrent outburst floods and active volcanism in Icelandic lacustrine settings during dynamic Younger Dryas-Early Holocene deglaciation, Journal of Quaternary Research, 37, 1006-1023, https://doi.org/10.1002/jqs.3344, 2022.

Geirsdóttir, Á., Miller, G. H., Larsen, D. J., and Ólafsdóttir, S.: Abrupt Holocene climate transitions in the northern North Atlantic recorded by synchronized lacustrine records in Iceland, Quaternary Science Reviews, 70, 48-62, https://doi.org/10.1016/j.quascirev.2013.03.010, 2013.

Geirsdóttir, Á., Miller, G. H., Thordarson, T., Ólafsdóttir, K. B.: A 2000 year record of climate variations reconstructed from Haukadalsvatn, West Iceland, Journal of Paleolimnology, 41, 95-115, https://doi.org/10.1007/s10933-008-9253-z, 2009.

Gerrard, J.: An assessment of some of the factors involved in recent landscape change in Iceland. In: Maizels, J. K., and Caseldine, C. (Eds.), Environmental Change in Iceland Past and Present. Dordrecht, the Netherlands: Kluwer, pp. 237-253, 1991.

Grönvold, K., Óksarsson, N., Johnsen, S.J., Clausen, H. B., Hammer, C. U., Bond, C., and Bard, E.: Ash layers from Iceland in the Greenland GRIP ice core correlated with oceanic and land sediments, Earth and Planetary Science Letters, 135, 149-155, https://doi.org/10.1016/0012-821X(95)00145-3, 1995.

Gudmundsdóttir, E. R., Larsen, G., Björck, S., Ingólfsson, Ó., and Striberger, J.: A new high-resolution Holocene tephra stratigraphy in eastern Iceland: improving the Icelandic and North Atlantic tephrochronology, Quaternary Science Reviews, 150, 234-249, https://doi.org/10.1016/j.quascirev.2016.08.011, 2016.

Gudmundsdóttir, E. R., Larsen, G., and Eiríksson, J.: Two new Icelandic tephra markers: the Hekla Ö tephra layer, 6060 cal. yr BP, and Hekla DH tephra layer, ~6650 cal. yr BP. Land-sea correlation of mid-Holocene tephra markers, The Holocene, 21, 629–639, https://doi.org/10.1177/0959683610391313, 2011.

Gudmundsdóttir, E. R., Schomacker, A., Brynjólfsson, S., Ingólfsson, Ó., and Larsen, N. K.: Holocene tephrostratigraphy in Vestfirðir, NW, Iceland, Journal of Quaternary Science, 33, 827-839, https://doi.org/10.1002/jqs.3063, 2018.

Hagstofa Íslands: Talnagrunnur, https://px.hagstofa.is/pxen/pxweb/en/, 2024.

Hallsdóttir, M.: Pollen analytical studies of human influence on vegetation in relation to the Landn?am tephra layer in southwest Iceland, Lundqua Thesis 18, 45, 1987.

Hallsdóttir, M.: On the pre-settlement history of Icelandic vegetation, Icelandic Agricultural Sciences, 9, 17-29, 1995.

Hallsdóttir, M., and Caseldine, C.J.: The Holocene vegetation history of Iceland, state-of- the-art and future. In: Caseldine, C., Russell, A., Hardardóttir, J., and Knudsen, O. (eds.) Iceland-Modern Processes and Past Environments, 5, 319, 2005.

Hanna, E., Jónsson, T., and Box, J. E.: An analysis of Icelandic climate since the nineteenth century, International Journal of Climatology, 24, 1193-1210, https://doi.org/10.1002/joc.1051, 2004.

Hannesdóttir, H., Björnsson, H., Pálsson, F., Aðalgeirsdóttir, G., and Guðmundsson, S.: Variations of southeast Vatnajökull ice cap (Iceland) 1650-1900 and reconstruction of the glacier surface geometry at the Little Ice Age maximum, Geografiska Annaler: Series A Physical Geography, 97, 237-264, https://doi.org/10.1111/geoa.12064, 2015.

Hannesdóttir, H., Sigurðsson, O., Þrastarson, R. H., Guðmundsson, S., Belart, J. M. C., Pálsson, F., Magnússon, E., Víkingsson, S., Kaldal, I., and Jóhannesson, T.: A national inventory and variations in glacier extent in Iceland from the Little Ice Age maximum to 2019, Jökull, 70, 1-34, https://doi.org/10.33799/jokull2020.70.001, 2020.

Harðarson, B. S., Fitton, J. G., and Hjartarson, Á.: Tertiary volcanism in Iceland, Jökull, 58, 161-178, http://doi.org/10.33799/jokull208.58.161, 2008.

1075    Harning, D. J., Curtin, L., Geirsdóttir, Á., D'Andrea, W. J., Miller, G. H., and Sepúlveda, J.: Lipid biomarkers quantify Holocene summer temperature and ice cap sensitivity in Icelandic lakes, Geophysical Research Letters, 47, e2019GL085728, https://doi.org/10.1029/2019GL085728, 2020.

Harning, D. J., Geirsdóttir, Á., Miller, G. H., and Anderson, L. S.: Episodic expansion of Drangajökull, Vestfirðir, Iceland
1080    over the last 3 ka culminating in its maximum dimension during the Little Ice Age, Quaternary Science Reviews, 152, 118-131, https://doi.org/10.1016/j.quascirev.2016.10.001, 2016a.

Harning, D. J., Geirsdóttir, Á., Miller, G. H., and Zalzal, K.: Early Holocene deglaciation of Drangajökull, Vestfirðir, Iceland, Quaternary Science Reviews, 153, 192-198, https://doi.org/10.1016/j.quascirev.2016.09.030, 2016b.
1085

Harning, D. J., Geirsdóttir, Á., Miller, G. H.: Punctuated Holocene climate of Vestfirðir, Iceland, linked to internal/external variables and oceanographic conditions, Quaternary Science Reviews, 189, 31-42, https://doi.org/10.1016/j.quascirev.2018.04.009, 2018a.

1090    Harning, D. J., Jennings, A. E., Köseoğlu, D., Belt, S. T., Geirsdóttir, Á., and Sepúlveda, J.: Response of biological productivity to North Atlantic marine front migration during the Holocene, Climate of the Past, 17, 379-396, https://doi.org/10.5194/cp-17-379-2021, 2021.

Harning, D. J., Sacco, S., Anamthawat-Jónsson, K., Ardenghi, N., Thordarson, T., Raberg, R. H., Sepúlveda, J., Geirsdóttir,
1095    Á., Shapiro, B., Miller, G. H.: Delayed postglacial colonization of *Betula* in Iceland and the circum North Atlantic, eLife, 12, 1-23, https://doi.org/10.7554/eLife.87749.3, 2023.

Harning, D. J., Thordarson, T., Geirsdóttir, Á., Miller, G. H., and Florian, C. R.: Repeated Early Holocene eruptions of Katla, Iceland, limit the temporal resolution of the Vedde Ash, Bulletin of Volcanology, 86, 2, https://doi.org/10.1007/s00445-023-
1100    01690-9, 2024.

Harning, D. J., Thordarson, T., Geirsdóttir, Á., Miller, G. H., and Ólafsdóttir, S.: Marker tephra in Haukadalsvatn lake sediment: A key to the Holocene tephra stratigraphy of Northwest Iceland, Quaternary Science Reviews, 219, 154-170, https://doi.org/10.1016/j.quascirev.2019.07.019, 2019.
1105

Harning, D. J., Thordarson, T., Geirsdóttir, Á., and Zalzal, K.: Provenance, stratigraphy and chronology of Holocene tephra from Vestfirðir, Iceland, Quaternary Geochronology, 46, 59-76, https://doi.org/10.1016/j.quageo.2018.03.007, 2018b.

Holmes, N., Langdon, P. G., Caseldine, C. J., Wastegård, S., Leng, M. J., Croudace, I. W., and Davies, S. M.: Climatic variability during the last millennium in Western Iceland from lake sediment records, The Holocene, 26, 756–771, https://doi.org/10.1177/0959683615618260, 2016.

Janebo, M. H., Thordarson, T., Houghton, B. F., Bonadonna, C., Larsen, G., and Carey, R. J.: Dispersal of key subplinian-Plinian tephras from Hekla volcano, Iceland: implications for eruption source parameters, Bulletin of Volcanology, 78, 1-16, https://doi.org/10.1007/s00445-016-1059-7, 2016.

Jennings, A. E., Andrews, J. T., Pearce, C., Wilson, L., Ólafsdóttir, S.: Detrital carbonate peaks on the Labrador shelf, a 13-7 ka template for freshwater forcing from the Hudson Strait outlet of the Laurentide Ice Sheet into the subpolar gyre, Quaternary Science Reviews, 107, 62-80, https://doi.org/10.1016/j.quascirev.2014.10.022, 2015.

Jennings, A. E., Thordarson, T., Zalzal, K., Stoner, J., Hayward, C., Geirsdóttir, Á., and Miller, G. H.: Holocene tephra from Iceland and Alaska in SE Greenland Shelf Sediments. In: Austin, W.E.N., Abbott, P.M., Davies, S.M., Pearce, N.J.G., and Wastegård, S. (eds) *Marine Tephrochronology*. Geological Society, London, Special Publications, 398, 2014.

Jóhannsdóttir, G. E.: Mid-Holocene to late glacial tephrochronology in west Iceland as revealed in three lacustrine environments. MS thesis, University of Iceland, 2007.

Kluger, M. O., Lowe, D. J., Moon, V. G., Chaneva, J., Johnston, R., Villamor, P., Ilanko, T., Melchert, R. A., Orense, R. P., Loame, R. C., and Ross, N.: Seismically-induced down-saggin structures in tephra layers (tephra-seismites) preserved in lakes since 17.5 cal ka, Hamilton lowlands, New Zealand, Sedimentary Geology, 445, 106327, https://doi.org/10.1016/j.sedgeo.2022.106327, 2023.

Kristjánsdóttir, G. B., Moros, M., Andrews, J. T., and Jennings, A. E.: Holocene Mg/Ca, alkenones, and light stable isotope measurements on the outer North Iceland shelf (MD99–2269): A comparison with other multi-proxy data and sub-division of the Holocene, The Holocene, 26, 55–62, https://doi.org/10.1177/0959683616652703, 2017.

Kristjánsdóttir, G. B., Stoner, J. S., Jennings, A. E., Andrews, J. T., and Grönvold, K.: Geochemistry of Holocene cryptotephras from the North Iceland Shelf (MD99-2269): intercalibration with radiocarbon and palaeomagnetic chronostratigraphies, The Holocene 17, 155-176, https://doi.org/10.1177/0959683607075829, 2007.

Lacasse, C.: Influence of climate variability on the atmospheric transport of Icelandic tephra in the subpolar North Atlantic, Global Planetary Change, 29, 31-55, https://doi.org/10.1016/S0921-8181(01)00099-6, 2001.

Langdon, P. G., and Barber, K. E.: New Holocene tephras and a proxy climate record from a blanket mire in northern Skye, Scotland, Journal of Quaternary Science, 16, 753-759, https://doi.org/10.1002/jqs.655, 2001.

Langdon, P. G., Leng, M. J., Holmes, N., and Caseldine, C. J.: Lacustrine evidence of early-Holocene environmental change in northern Iceland: a multiproxy palaeoecology and stable isotope study, The Holocene, 20, 205-214, https://doi.org/10.1177/0959683609354301, 2010.

Larsen, D. J., Miller, G. H., Geirsdóttir, Á., and Ólafsdóttir, S.: Non-linear Holocene climate evolution in the North Atlantic: a high-resolution, multi-proxy record of glacier activity and environmental change from Hvítárvatn, central Iceland, Quaternary Science Reviews, 39, 14-25, https://doi.org/10.1016/j.quascirev.2012.02.006, 2012.

Larsen, D. J., Miller, G. H., Geirsdóttir, Á., and Thordarson, T.: A 3000-year varved recoed of glacier activity and climate change form the proglacial lake Hvítárvatn, Iceland, Quaternary Science Reviews, 30, 2715-2731, https://doi.org/10.1016/j.quascirev.2011.05.026, 2011.

Larsen, G.: Gjóskulagid úr Heklugosinu 1158 (The tephra layer from the 1158 AD eruption of Hekla). Jardfrædafélag Islands, Vorrádstefna, Yfirlit og Ágrip. Geoscience Society of Iceland, Reykjavík: 25–27, 1992.

Larsen, G., Dugmore, A. J., and Newton, A. J.: Geochemistry of historical-age silicic tephras in Iceland, The Holocene, 9, 463-471, https://doi.org/10.1191/095968399669624108, 1999.

Larsen, G., and Eiríksson, J.: Holocene tephra archives and tephrochronology in Iceland – a brief overview, Jökull, 58, 229-250, http://doi.org/10.33799/jokull2008.58.229, 2008.

Larsen, G., Eiríksson, J., Knudsen, K. L., and Heinemeier, J.: Correlation of late Holocene terrestrial and marine tephra markers, north Iceland: implications for reservoir age changes, Polar Research, 21, 283-290, https://doi.org/10.3402/polar.v21i2.6489, 2002.

Larsen, G., Newton, A. J., Dugmore, A. J., Vilmundardóttir, E. G.: Geochemistry, dispersal, volumes and chronology of Holocene silicic tephra layers from the Katla volcanic system, Iceland, Journal of Quaternary Science, 16, 119-132, https://doi.org/10.1002/jqs.587, 2001.

1175

Larsen, G., Róbertsdóttir, B. G., Óladóttir, B. A., and Eiríksson, J.: A shift in eruption mode of Hekla volcano, Iceland, 3000 years ago: two-coloured Hekla tephra series, characteristics, dispersal and age, Journal of Quaternary Science, 35, 143-154, https://doi.org/10.1002/jqs.3164, 2020.

1180 Larsen, G., and Thórarinsson, S.: H-4 and other acid Hekla tephra layers, Jökull, 27, 27-46, 1977.

Lavaud, J., Rousseau, B., van Gorkom, H. J., and Etienne, A.-L: Influence of the diadinoxanthin pool size on photoprotection in the marine planktonic diatom *Phaeodactylum tricornutum*, Plant Physiology, 129, 1398–1406, https://doi.org/10.1104/pp.002014, 2002.

Lawson, I. T., Gathorne-Hardy, F. J., Church, M. J., Newton, A. J., Edwards, K. J., Dugmore, A. J., and Einarsson, Á.:
1185 Environmental impacts of the Norse settlement: Palaeoenvironmental data from Mývatnssveit, northern Iceland, Boreas, 36,1–19, https://doi.org/10.1111/j.1502-3885.2007.tb01176.x, 2007.

Lawson, I. T., Swindles, G. T., Plunkett, G., and Greenberg, D.: The spatial distribution of Holocene cryptotephras in north-west Europe since 7 ka: implications for understanding ash fall events from Icelandic eruptions, Quaternary Science Reviews,
1190 41, 57-66l, https://doi.org/10.1016/j.quascirev.2012.02.018, 2012.

Leavitt, P. R., and Hodgson, D. A.: Sedimentary pigments. In: Smol, J. P., H. J. B. Birks and W. M. Last (eds.), Tracking Environmental Change using Lake Sediments. Volume 3: Terrestrial, Algal and Siliceous Indicators. Kluwer Academic Publishers, Dordrecht. The Netherlands, 295-325, 2001.

Lowe, D. J.: Tephrochronology and its application: A review, Quaternary Geochronology, 6, 107-153,
1195 https://doi.org/10.1016/j.quageo.2010.08.003, 2011.

Mangerud, J., Furnes, H., and Jóhansen, J.: A 9000-year-old ash bed on the Faroe Islands, Quaternary Research, 26, 262-265, https://doi.org/10.1016/0033-5894(86)90109-2, 1986.

1200 Mangerud, J., Lie, S.E., Furnes, H., Kristiansen, I. L., and Lømo, L.: A Younger Dryas Ash bed in Western Norway, and its possible correlations with tephra in cores from the Norwegian Sea and the North Atlantic, Quaternary Research, 21, 85-104, https://doi.org/10.1016/0033-5894(84)90092-9, 1984.

Marshall, J., Kushnir, Y., Battisti, D., Chang, P., Czaja, A., Dickson, R., Hurrell, J., McCartney, M., Saravanan, R., and Visbeck, M.: North Atlantic climate variability: phenomena, impacts and mechanisms, International Journal of Climatology, 21, 1863-1898, https://doi.org/10.1002/joc.693, 2001.

McMurdie, P. J., and Holmes, S.: phyloseq: An R package for reproducible interactive analysis and graphics of microbiome census data, PLoS ONE 8, e61217, http://dx.plos.org/10.1371/journal.pone.0061217, 2013.

Möckel, S. C., Erlendsson, E., Prater, I., and Gísladóttir, G.: Tephra deposits and carbon dynamics in peatlands of a volcanic region – lessons from the Hekla 4 eruption, Land Degradation and Development, 32, 654-669, https://doi.org/10.1002/ldr.3733, 2021.

Moossen, H., Bendle, J., Seki, O., Quillmann, U., and Kawamura, K.: North Atlantic Holocene climate evolution recorded by high-resolution terrestrial and marine biomarker records, Quaternary Science Reviews, 129, 111–127, https://doi.org/10.1016/j.quascirev.2015.10.013, 2015.

Óladóttir, B. A., Larsen, G., Thordarson, T., and Sigmarsson, O: The Katla volcano S-Iceland: Holocene tephra stratigraphy and eruption frequency, Jökull, 55, 53-74, http://doi.org/10.33799/jokull2005.55.053, 2005.

Óladóttir, B. A., Thordarson, T., Larsen, G., and Sigmarsson, O.: Survival of the Mýrdalsjökull ice cap through the Holocene thermal maximum: evidence from sulfur contents in Katla tephra layers (Iceland) from the last ~8400 years, Annals of Glaciology, 45, 183-188, https://doi.org/10.3189/172756407782282516, 2007.

Óladóttir, B. A., Larsen, G., and Sigmarsson, O.: Holocene volcanic activity at Grímsvötn, Bárdarbunga and Kverkfjöll subglacial centres beneath Vatnajökull, Iceland, Bulletin of Volcanology, 73, 1187-1208, https://doi.org/10.1007/s00445-011-0461-4, 2011.

Óladóttir, B. A., Thordarson, T., Geirsdóttir, Á., Jóhannsdóttir, G. E., and Mangerud, J.: The Saksunarvatn Ash and the G10ka series tephra. Review and current state of knowledge, Quaternary Geochronology, 56, 101041, https://doi.org/10.1016/j.quageo.2019.101041, 2020.

Ólafsdóttir, S., Geirsdóttir, Á., Miller, G. H., Stoner, J. S., and Channell, J. E. T.: Synchronizing Holocene lacustrine and marine sediment records using paleomagnetic secular variation, Geology, 41, 535-538, https://doi.org/10.1130/G33946.1, 2013.

Paerl, H. W., and Paul, V. J.: Climate change: Links to global expansion of harmful cyanobacteria, Water Research, 46, 1349-1363, https://doi.org/10.1016/j.watres.2011.08.002, 2012.

1240

Patton, H., Hubbard, A., Bradwell, T., and Schomacker, A.: The configuration, sensitivity and rapid retreat of the Late Weichselian Icelandic ice sheet, Earth-Science Reviews, 166, 223-245, https://doi.org/10.1016/j.earscirev.2017.02.001, 2017.

Pilcher, J. R., Hall, V. A., and McCormac, F. G.: Dates of Holocene Icelandic volcanic eruptions from tephra layers in Irish
1245    peats, The Holocene, 5, 103-110, https://doi.org/10.1177/095968369500500111, 1995.

Pilcher, J. R., Hall, V. A., and McCormac, F. G.: An outline tephrochronology for the Holocene of the north of Ireland, Journal of Quaternary Science, 11, 485-494, https://doi.org/10.1002/(SICI)1099-1417(199611/12)11:6<485::AID-JQS266>3.0.CO;2-T, 1996.

1250

Quillmann, U., Marchitto, T. M., Jennings, A. E., Andrews, J. T., and Friestad, B. F.: Cooling and freshening at 8.2 ka on the NW Iceland Shelf recorded in paired $\delta^{18}O$ and Mg/Ca measurements of the benthic foraminifer *Cibicides lobatulus*, Quaternary Research, 78, 528-539, https://doi.org/10.1016/j.yqres.2012.08.003, 2012.

1255    Rasmussen, S. O., Andersen, K. K., Svensson, A. M., Steffensen, J. P., Vinther, B. M., Clausen, H. B., Siggaard-Andersen, M.-L., Johnsen, S. J., Larsen, L. B., Dahl-Jensen, D., Bigler, M., Röthlisberger, R., Fischer, H., Goto-Azuma, K., Hansson, M. E., and Ruth, U.: A new Greenland ice core chronology for the last glacial termination, Journal of Geophysical Research, 111, 1-16, https://doi.org/10.1029/2005JD006079, 2006.

1260    R Core Team: R: A language and environment for statistical computing. Vienna, Austria: R Foundation for Statistical Computing, https://www.R-project.org/, 2021.

Reimer, P. J., Austin, W. E. N., Bard, E., Bayliss, A., Blackwell, P. G., Bronk Ramsey, C., Butzin, M., Cheng, H., Edwards, R. L., Friedrich, M., Grootes, P. M., Guilderson, T. P., Hajdas, I., Heaton, T. J., Hogg, A. G., Hughen, K. A., Kromer, B.,
1265    Manning, S. W., Muscheler, R., Palmer, J. G., Pearson, C., van der Plicht, J., Reimer, R. W., Richards, D. A., Scott, E. M., Southon, J. R., Turney, C. S. M., Wacker, L., Adolphi, F., Büntgen, U., Capano, M., Fahrni, S. M., Fogtmann-Schulz, A., Friedrich, R., Köhler, P., Kudsk, S., Miyake, F., Olsen, J., Reinig, F., Sakamoto, M., Sookdeo, A., and Talamo, S.: The IntCal20 northern hemisphere radiocarbon age calibration curve (0-55 cal kBP), Radiocarbon, 62, 725-757, https://doi.org/10.1017/RDC.2020.41, 2020.

1270

Richter, N., Russell, J. M., Garfinkel, J., and Huang, Y.: Winter-spring warming in the North Atlantic during the last 2000 years: evidence from southwest Iceland, Climate of the Past, 17, 1363-1383, https://doi.org/10.5194/cp-17-1363-2021, 2020.

Rohling, E. J., and Pälike, H.: Centennial-scale climate cooling with a sudden cold event around 8,200 years ago, Nature, 434, 975-979, https://doi.org/10.1038/nature03421, 2005.

1275 Rousseau, V., Leynaert, A., Daoud, N., and Lancelot, C.: Diatom succession, silicification and silicic acid availability in Belgian coastal waters (Southern North Sea), Marine Ecology Progress Series, 236, 61–73, http://doi.org/meps236061, 2002.

Rundgren, M.: Biostratigraphic evidence of the Allerød-Younger Dryas-Preboreal Oscillation in Northern Iceland, Quaternary Research, 44, 405-416, https://doi.org/10.1006/qres.1995.1085, 1995.

1280 Rundgren, M.: Early Holocene vegetation of northern Iceland: pollen and plant macrofossil evidence from the Skagi peninsula, The Holocene, 5, 553-564, https://doi.org/10.1191/095968398669995117, 1998.

Rundgren, M., and Ingólfsson, Ó.: Plant survival in Iceland during periods of glaciation?, Journal of Biogeography, 26, 387-396, https://doi.org/10.1046/j.1365-2699.1999.00296.x, 1999.

1285

Rundgren, M., Ingólfsson, Ó., Björck, S., Jiang, H., and Haflidason, H.: Dynamic sea-level change during the last deglaciation of northern Iceland, Boreas, 26, 201-215, https://doi.org/10.1111/j.1502-3885.1997.tb00852.x, 1997.

Simkin, A. J., Kapoor, L., Doss, C. G. P., Hofmann, T. A., Lawson, T., and Ramamoorthy, S.: The role of photosynthesis
1290 related pigments in light harvesting, photoprotection and enhancment of photosynthetic yield in planta, Photosynthesis Research, 152, 23-42, https://doi.org/10.1007/s11120-021-00892-6, 2022.

Smith, K. P.: Landnam: The settlement of Iceland in archaeological and historical perspective, World Archaeology, 26, 319-347, https://doi.org/10.1080/00438243.1995.9980280, 1995.

Smith, V. H.: Nutrient dependence of primary productivity in lakes, Limnology and Oceanography, 24, 1051–1064,
1295 https://doi.org/10.4319/lo.1979.24.6.1051, 1979.

Smol, J. P., and Cumming, B. F.: Tracking long-term changes in climate using algal indicators in lake sediments, Journal of Phycology, 1011, 986–1011, https://doi.org/10.1046/j.1529-8817.2000.00049.x, 2000.

Stoner, J. S., Channell, J. E. T., Mazaud, A., Strano, S. E., Xuan, C.: The influence of high-latitude flux lobes on the Holocene paleomagnetic record of IODP Site U1305 and the northern North Atlantic, Geochemistry, Geophysics, Geosystems, 14, 4623-4646, https://doi.org/10.1002/ggge.20272, 2013.

Stoner, J. S., Jennings, A., Kristjánsdóttir, G. B., Dunhill, G., Andrews, J. T., and Hardardóttir, J.: A paleomagnetic approach toward refining Holocene radiocarbon-based chronologies: Paleoceanographic records from the north Iceland (MD99-2269) and east Greenland (MD99-2322) margins, Paleoceanography, 22, 1-23, https://doi.org/10.1029/2006PA001285, 2007.

Storm, G.: Annales Reseniani. Islandske Annaler: indtil 1578. Kristjanía: Norsk historisk kildeskriftfond, 27, 1977a.

Storm, G.: Flatbøgens Annaler Islandske Annaler: indtil 1578. Kristjanía: Norsk historisk kildeskriftfond, 534, 1977b.

Storm, G.: Skálholts-Annaler Islandske Annaler: indtil 1578. Kristjanía: Norsk historisk kildeskriftfond, 193, 1977c.

Stramski, D., Sciandra, A., and Claustre, H.: Effects of temperature, nitrogen, and light limitation on the optical properties of the marine diatom *Thalassiosira pseudonana*, Limnology and Oceanography, 47, 392–403, https://doi.org/10.4319/lo.2002.47.2.0392, 2002.

Streeter, R., Dugmore, A. J., Lawson, I. T., Erlendsson, E., and Edwards, K. J.: The onset of the palaeoanthropocene in Iceland: changes in complex natural systems, The Holocene, 25, 1662-1675, https://doi.org/10.1177/0959683615594468, 2015.

Striberger, J., Björck, S., Holmgren, S., and Hamerlík, L.: The sediments of Lake Lögurinn e a unique proxy record of Holocene glacial meltwater variability in eastern Iceland, Quaternary Science Reviews 38, 76-88, https://doi.org/10.1016/j.quascirev.2012.02.001, 2012.

Skrzypek, G., Paul, D., and Wojtun, B.: Stable isotope composition of plants and peat from Arctic mire and geothermal area in Iceland, Polar Research, 29, 365-376, 2008.

Telford, R. J., Barker, P., Metcalfe, S., and Newton, A.: Lacustrine responses to tephra deposition: examples from Mexico, Quaternary Science Reviews, 23, 23-24, https://doi.org/10.1016/j.quascirev.2004.03.014, 2004.

Thórarinsson, S.: Tefrokronoliska studier pa Island (Tephrochronological studies in Iceland), Geogr. Ann. 26, 1-217, 1944.

Tierney, J. E., Poulsen, C. J., Montañez, I. P., Bhattacharya, T., Feng, R., Ford, H. L., Hönisch, B., Inglis, G. N., Petersen, S. V., Sagoo, N., Tabor, C. R., Thirumalai, K., Zhu, J., Burls, N. J., Foster, G. L., Goddéris, Y., Huber, B. T., Ivany, L. C., Turner, S. K., Lunt, D. J., McElwain, J. C., Mills, B. J. W., Otto-Bliesner, B. L., Ridgwell, A., and Zhang, Y. G.: Past climates inform our future, Science, 370, 680, http://doi.org/10.1126/science.aay3701, 2020.

Thórarinsson, S.: Tefrokronoliska studier pa Island (Tephrochronological studies in Iceland), Geografiska Annaler, 26, 1–217, 1944.

Thórarinsson, S.: Uppblástur á Íslandi í ljósi öskulaga-rannsókna, Ársrit Skógræktarfélag Íslands, Reykjavík, 17-54, 1961.

Thórarinsson, S.: The eruptions of Hekla in historical times: a tephrochronological study. In: Einarsson, T., Kjartansson, G., Thorarinsson, S. (eds) *The eruption of Hekla 1947-1948*. Societas Scientiarum Islandica, Reykjavik, 1-177, 1967.

Thordarson, T., and Larsen, G.: Volcanism in Iceland in historical time: volcano types, eruption styles and eruptive history, Journal of Geodynamics, 43, 118–152, https://doi.org/10.1016/j.jog.2006.09.005, 2007.

Thordarson, T., and Höskuldsson, Á.: Postglacial volcanism in Iceland, Jökull, 58, 197-228, http://doi.org/10.33799/jokull2008.58.197, 2008.

Thordarson, T., Self, S., Óskarsson, N., and Hulsebosch, T.: Sulphur, chlorine, and fluorine degassing and atmospheric loading by the 1783-1784 AD Laki (Skaftár Fires) eruption in Iceland, Bulletin of Volcanology, 58, 205-225, http://doi.org/10.1007/s004450050136, 1996.

Timms, R. G. O., Matthews, I. P., Palmer, A. P., and Candy, I.: Toward a tephrostratigraphic framework for the British Isles: A Last Glacial to Interglacial Transition (LGIT c. 16-8 ka) case study from Crudale Meadow, Orkney, Quaternary Geochronology, 46, 28-44, https://doi.org/10.1016/j.quageo.2018.03.008, 2018.

Timms, R. G. O., Matthews, I. P., Palmer, A. P., Candy, I., and Abel, L.: A high-resolution tephrostratigraphy from Quoyloo Meadow, Orkney, Scotland: Implications for the tephrostratigraphy of NW Europe during the Last Glacial-Interglacial Transition, Quaternary Geochronology, 40, 67-81, https://doi.org/10.1016/j.quageo.2016.06.004, 2017.

Tinganelli, L., Erlendsson, E., Eddudóttir, S. D., and Gísladóttir, G.: Impacts of climate, tephra, and land use upon Holocene landscape stability in Northwest Iceland, Geomorphology, 322, 117-131, https://doi.org/10.1016/j.geomorph.2018.08.025, 2018.

van den Bogaard, C., Dorfler, W., Sandgren, P., and Schmincke, H.-U.: Correlating the Holocene records: Icelandic Tephra found in Schleswig-Holstein (Northern Germany), Naturwissenschaften, 81, 554-556, https://doi.org/10.1007/BF01140005, 1994.

van den Bogaard, C., Dorfler, W., Glos, R., Nadeau, M.-J., Grootes, P. M., and Erlenkeuser, H.: Two tephra layers bracketing late Holocene paleoecological changes in northern Germany, Quaternary Research, 57, 314-324, https://doi.org/10.1006/qres.2002.2325, 2002.

Vésteinsson, O., and McGovern, T.: The peopling of Iceland, Norwegian Archaeological Review, 45, 206-218, https://doi.org/10.1080/00293652.2012.721792, 2012.

Vogel, H., Rósen, P., Wagner, B., Melles, M., and Persson, P.: Fourier transform infrared spectroscopy, a new cost-effective tool for quantitative analysis of biogeochemical properties in long sediment records, Journal of Paleolimnology, 40, 689-702, https://doi.org/10.1007/s10933-008-9193-7, 2008.

Walker, G. P. L., and Croasdale, R.: Characteristics of some basaltic pyroclasts, Bulletin of Volcanology, 35, 303-317, https://doi.org/10.1007/BF02596957, 1972.

Wang, Y., and Wooller, M.: The stable isotopic (C and N) composition of modern plants and lichens from northern Iceland: with ecological and paleoenvironmental implications, Jökull, 56, 27-38, http:doi.org/10.33799/jokull2006.56.027, 2006.

Wastegård, S., Björck, S., Grauert, M., and Hannon, G. E.: The Mjáuvøtn tephra and other Holocene tephra horizons from the Faroe Islands: a link between the Icelandic source region, the Nordic Seas, and the European continent, The Holocene, 11, 101-109, https://doi.org/10.1191/095968301668079904, 2001.

Wastegård, S., Rundgren, M., Schoning, K., Andersson, S., Björck, S., Borgmark, A., and Possnert, G.: Age, geochemistry and distribution of the mid-Holocene Hekla-S/Kebister tephra, The Holocene, 18, 539-549, https://doi.org/10.1177/0959683608089208, 2008.

Wastegård, S., Gudmundsdóttir, E. R., Lind, E. M., Timms, R. G. O., Björck, S., Hannon, G. E., Olsen, J., and Rundgren, M.: Towards a Holocene tephrochronology for the Faroe Islands, North Atlantic, Quaternary Science Reviews, 195, 195-214, https://doi.org/10.1016/j.quascirev.2018.07.024, 2018.

Wunsch, C.: Meridional heat flux of the north Atlantic Ocean, Proceedings of the National Academy of Sciences, 77, 5043-5047, https://doi.org/10.1073/pnas.77.9.5043, 1980.

1400

Xiao, X., Zhao, M., Knudsen, K.L., Sha, L., Eiríksson, J., Gudmundsdóttir, E., Jiang, H., and Guo, Z.: Deglacial and Holocene sea-ice variability north of Iceland and response to ocean circulation changes, Earth and Planetary Science Letters, 472, 14-24, https://doi.org/10.1016/j.epsl.2017.05.006, 2017.